

Experimental warming leads to convergent succession of grassland archaeal community

Received: 29 August 2022

Accepted: 3 April 2023

Published online: 04 May 2023

 Check for updates

Ya Zhang ¹, Daliang Ning ¹, Linwei Wu^{1,2}, Mengting Maggie Yuan ^{1,3}, Xishu Zhou^{1,4}, Xue Guo⁵, Yuanliang Hu ^{1,6}, Siyang Jian ¹, Zhifeng Yang ¹, Shun Han ¹, Jiajie Feng¹, Jialiang Kuang ¹, Carolyn R. Cornell ¹, Colin T. Bates¹, Yupeng Fan ¹, Jonathan P. Michael¹, Yang Ouyang¹, Jiajing Guo^{1,7}, Zhipeng Gao ^{1,8}, Zheng Shi¹, Naijia Xiao¹, Ying Fu¹, Aifen Zhou ¹, Liyou Wu ¹, Xueduan Liu⁴, Yunfeng Yang ⁵, James M. Tiedje ⁹ & Jizhong Zhou ^{1,10,11,12} ✉

Understanding the temporal succession of ecological communities and the underlying mechanisms in response to climate warming is critical for future climate projections. However, despite its fundamental importance in ecology and evolution, little is known about how the Archaea domain responds to warming. Here we showed that experimental warming of a tallgrass prairie ecosystem significantly altered the community structure of soil archaea and reduced their taxonomic and phylogenetic diversity. In contrast to previous observations in bacteria and fungi, we showed convergent succession of the soil archaeal community between warming and control. Although stochastic processes dominated the archaeal community, their relative importance decreased over time. Furthermore, the warming-induced changes in the archaeal community and soil chemistry had significant impacts on ecosystem functioning. Our results imply that, although the detrimental effects of biodiversity loss on ecosystems could be much severer, the soil archaeal community structure would be more predictable in a warmer world.

Since its formal recognition in 1990 (ref. 1), the Archaea domain has challenged our views on the diversity, ecology and evolution of life, yet it remains the least understood². In contrast to the traditional wisdom that archaea prefer extreme environments^{3–5}, archaea are prominent members of all terrestrial and marine communities², and are abundant

in water columns, ocean sediments and soils^{5,6}. Possessing unusual physiologies^{2,7}, they play central roles in mediating global carbon (C), nitrogen (N) and sulfur (S) cycles^{8–10}. They are also an important component of the human microbiome, although their role in health and disease remains undetermined¹¹. Furthermore, the recent discovery

¹Institute for Environmental Genomics and Department of Microbiology and Plant Biology, University of Oklahoma, Norman, OK, USA. ²Institute of Ecology, Key Laboratory for Earth Surface Processes of the Ministry of Education, College of Urban and Environmental Sciences, Peking University, Beijing, China. ³Department of Environmental Science, Policy, and Management, University of California, Berkeley, CA, USA. ⁴School of Minerals Processing and Bioengineering, Central South University, Changsha, Hunan, China. ⁵State Key Joint Laboratory of Environment Simulation and Pollution Control, School of Environment, Tsinghua University, Beijing, China. ⁶Hubei Key Laboratory of Edible Wild Plants Conservation and Utilization, College of Life Sciences, Hubei Normal University, Huangshi, China. ⁷Hunan Agriculture Product Processing Institute, Hunan Academy of Agricultural Sciences, Changsha, Hunan, China. ⁸College of Animal Science and Technology, Hunan Agricultural University, Changsha, Hunan, China. ⁹Center for Microbial Ecology, Michigan State University, East Lansing, MI, USA. ¹⁰School of Civil Engineering and Environmental Sciences, University of Oklahoma, Norman, OK, USA. ¹¹School of Computer Science, University of Oklahoma, Norman, OK, USA. ¹²Earth and Environmental Sciences, Lawrence Berkeley National Laboratory, Berkeley, CA, USA. ✉e-mail: jzhou@ou.edu

of the Asgard archaeal superphylum leads to a possibility of archaea as ancestors of eukaryotic life^{12–14}. Thus, understanding the physiology, ecology and evolution of archaea represents one of the most exciting frontiers in biology².

Despite such recent exciting discoveries, we have a limited understanding of archaea in terrestrial environments, particularly in soils^{6,15–18}. Archaea are ubiquitously present in soil, represent a mass of 0.5 Gt C (an amount comparable with 7 Gt C for soil bacteria)¹⁸, and are vital to soil nitrification and methanogenesis due to the high numbers of ammonia-oxidizing archaea (AOA) and methanogenic archaea^{19,20}. It was reported that their spatial distribution patterns in soils are distinct from those of soil bacteria^{6,15}, including their biodiversity distribution and ecological drivers^{6,15–17}. However, our understanding of the responses of soil archaea to climate change remains rudimentary^{21–24}.

Climate warming represents one of the biggest disturbance factors imposed on human society and global ecosystems. As temperature is a major driver of biological processes, climate warming will impact various ecological communities. On the basis of long-term time-series data, our previous studies revealed that experimental warming leads to the divergent succession of soil bacterial and fungal communities²⁵, accelerates microbial temporal scaling²⁶, reduces the biodiversity of soil bacteria, fungi and protists²⁷, but increases bacterial network complexity and stability²⁸. However, how climate warming affects the temporal succession of the archaeal community remains elusive. On the one hand, since archaea and bacteria are both prokaryotic and share greater structural similarity²⁹, it is expected that climate warming could lead to the divergent succession of soil archaeal communities similarly as it does for bacteria and fungi. On the other hand, soil archaeal communities could exhibit distinct temporal responses to climate warming that are convergent or idiosyncratic³⁰ since archaea have unique physiology⁷.

Here we conducted a long-term in situ warming experiment in a native, tallgrass prairie ecosystem at the Kessler Atmospheric and Ecological Field Station (KAEFS) in the US Great Plains in Central Oklahoma (34° 59' N, 97° 31' W)^{25,31}. This long-term multifactor climate change experiment was established in 2009 with a split-block design, in which the warming treatment plots have been subjected to continuous +3 °C warming by infrared radiators and the control plots by 'dummy' infrared radiators to account for the shading effect³¹. In this study, we focus on the warming effects on soil archaeal community diversity and succession by determining: (1) whether and how warming affects the diversity and succession of soil archaeal community; (2) what the relative roles of deterministic and stochastic processes are in controlling the temporal dynamics of soil archaeal community in response to climate warming; and (3) whether and how warming-induced changes in the soil archaeal community mediate ecosystem functioning. We hypothesize that the soil archaeal community would undergo divergent succession under warming due to increased deterministic filtering effects over time, similar to what was observed for bacteria and fungi, and that decreases in the taxonomic and functional diversity of the soil archaeal community under warming would negatively impact linked ecosystem functions.

Impacts of warming on archaeal diversity

At the higher taxonomic levels, such as phylum and order, the soil archaeal community was primarily composed of Thaumarchaeota (Nitrososphaerales; ≥96.5% abundance, ≥41.3% incidence) and Euryarchaeota (Methanomassiliicoccales; -0.35% abundance, -2.1% incidence), and to a lesser extent of Pacearchaeota (unclassified), Woearchaeota (unclassified) and Crenarchaeota (unclassified) (Fig. 1a and Extended Data Fig. 1). The major Nitrososphaerales clade identified is potentially responsible for ammonia oxidation process³², and the Methanomassiliicoccales clade is potentially methanogenic³³.

To examine the warming effects on soil archaeal community diversity, linear mixed-effects models (LMM) were used, in which the

regression coefficients represent the directions and magnitudes of the warming effect, namely effect sizes (β). Warming had strong negative effects ($\beta = -0.64$ to -0.60 , $P < 0.008$) on archaeal richness and Faith's phylogenetic diversity (PD) (Fig. 1b), as richness decreased by 1.4% ($\beta = -0.64$, $P = 0.008$) and PD by 7.3% ($\beta = -0.60$, $P = 0.006$). Similarly, warming also marginally decreased the functional richness of the archaeal community as measured by a probe-based microarray GeoChip ($\beta = -0.17$, $P = 0.070$). However, such decreases in functional richness were not detected by metagenome EcoFUN-MAP (a method designed for annotating metagenomic sequences by comparing them with functional genes used to fabricate GeoChip) ($\beta = 0.14$, $P = 0.533$; Fig. 1b), which was most likely due to the inherent problems of lower reproducibility, quantitative capability and sensitivity associated with shotgun sequencing approaches^{34–36}. These results indicate that experimental warming significantly reduced soil archaeal biodiversity, consistent with the observations for bacteria, fungi and protists^{27,37–39}.

The warming effects on soil archaea varied considerably for individual operational taxonomic units (OTUs). Warming significantly decreased the relative abundance of Nitrososphaerales-affiliated OTU2 (response ratios (RR) = -0.45 ± 0.32 ; 9.1% under warming vs 14.3% under control; Supplementary Table 1) but increased the relative abundance of other Nitrososphaerales-affiliated taxa, including OTU4 (RR = 0.40 ± 0.27 ; 10.9% vs 7.4%) and OTU11 (RR = 0.75 ± 0.60 ; 1.3% vs 0.6%). Two rare Methanobacteriales-affiliated taxa (OTU1057 and OTU535) were significantly negatively impacted by warming (RR < -2.30 ; $<0.001\%$ under warming vs. 0.01% under control). These results suggest high variability even within the same taxonomic clade in responses to warming, consistent with our previous observations on the differential effects of warming on various microbial groups of bacteria and fungi²⁵.

Effects of warming on community structure and succession

As revealed by three complementary non-parametric multivariate statistical tests (Adonis, ANOSIM and MRPP), the overall archaeal community structure was significantly different ($P < 0.05$) between the warmed and control plots (Table 1 and Supplementary Table 2). Time also had significant ($P < 0.03$) effects on the soil archaeal community (Table 1). The detrended correspondence analysis (DCA) showed that the soil archaeal community structure was shifted over time by warming (Extended Data Fig. 2). Before starting the warming treatment in 2009, the soil samples from both warmed and control plots were closely clustered. In the subsequent years, the warmed samples were generally separated from the control samples on a yearly basis (Extended Data Fig. 2). Together, these results suggest that experimental warming significantly altered soil archaeal community structure and succession, which agrees with the results for bacteria and fungi observed in this site²⁵. Studies with plants have shown similar results, with climate warming impacting phylogenetic diversity of grassland plant communities³⁹, abundance within species ranges of trees⁴⁰ and local species extinctions of plants⁴¹.

The community differences between the paired warmed and control plots decreased significantly with time on the basis of both the Sorensen metric (Fig. 1c; slope = -0.009 , $P = 0.043$) and phylogenetic distance metric (Fig. 1c; slope = -0.013 , $P = 0.020$). In contrast, the corresponding community differences between warming and control increased with time for bacteria (Fig. 1c; slope = 0.011 , $P = 0.004$ for Sorensen metrics and slope = 0.009 , $P = 0.001$ for unweighted Unifrac metrics) and fungi (Extended Data Fig. 3; slope = 0.020 , $P = 0.007$ for Sorensen metrics and slope = 0.014 , $P = 0.003$ for unweighted Unifrac metrics). Also, both potential ammonia oxidizer (Nitrososphaerales) and the dominant methanogen (Methanomassiliicoccales) showed similar trends as the domain Archaea (Extended Data Fig. 4). In addition, the archaeal functional gene-based (*amoA* gene) community distances between warming and control decreased significantly ($P < 0.05$)

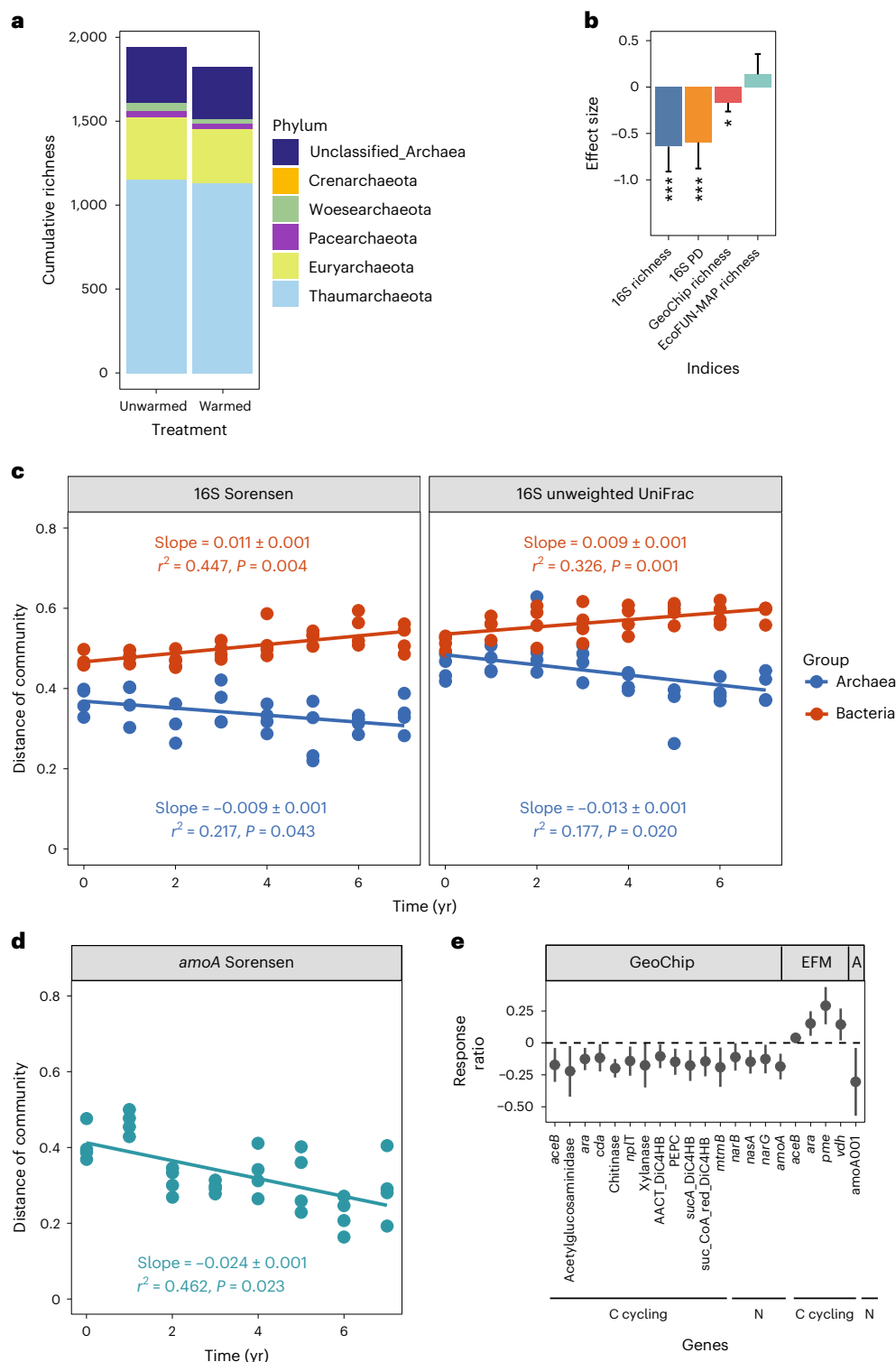


Fig. 1 | Effects of experimental warming on archaeal community diversity and succession across 7 yr. **a**, Archaeal community composition under unwarmed and warmed conditions. Cumulative richness is expressed as the number of OTUs. **b**, The effect sizes of warming on archaeal biodiversity (including taxonomic, phylogenetic and functional diversity). The estimated effect sizes (β) are regression coefficients based on rescaled response variables (with zero mean and unit standard deviation) in the LMMs. Bars represent mean \pm s.e.m. of effect sizes. Statistical significance is based on Wald type II χ^2 tests ($n = 64$; two-sided; $P = 0.008, 0.006, 0.070, 0.533$ for 16S richness, 16S PD, GeoChip richness and EcoFUN-MAP richness, respectively). *** $P < 0.01$; * $P < 0.10$. **c, d**, Temporal changes in community differences between warming and control conditions. **c**, 16S rRNA genes (left: Sorensen dissimilarity metrics; right: unweighted UniFrac dissimilarity metrics). **d**, *amoA* genes. The slopes of the archaeal community

and the bacterial community are significantly different in c ($P = 0.007$ and $P < 0.001$). The first year is 2009 (year 0). Considering the repeated-measures design, the warming-vs-control dissimilarity values at each block were fitted to LMMs with a fixed effect of time and a random intercept and slope effect among different pairs of plots (blocks). The slopes are presented as a coefficient in fixed effect \pm standard error in random effect. The r^2 values were calculated (details in Methods) to reflect the variance explained by the whole LMM model. P values were based on permutation tests (two-sided). The lines show the fixed effects of the LMM. **e**, Differences in functional gene abundances between warming and control by response ratios. Bars represent mean \pm 95% confidence interval of response ratios. Only genes showing significant differences between warming and control ($P < 0.05$, $n = 64$) are shown. EFM, metagenome EcoFUN-MAP; A, *amoA* genes (mean relative abundance $>10.0\%$).

Table 1 | Summary of permutational multivariate analysis of warming, year and block on soil archaea community structure

Variables	16S rRNA gene			GeoChip			Metagenome EcoFUN-MAP		
	F	R ²	P	F	R ²	P	F	R ²	P
Warming (W)	3.923	0.040	0.014	6.037	0.047	0.001	2.215	0.031	0.001
Year (Y)	3.877	0.274	0.001	8.857	0.485	0.001	1.922	0.189	0.001
Block (B)	2.277	0.069	0.026	1.847	0.043	0.031	1.194	0.050	0.071
Y×B	1.437	0.305	0.066	1.113	0.183	0.278	1.002	0.295	0.443

Permutational multivariate analysis of variance (Adonis) was used on the basis of Bray–Curtis dissimilarity matrices. The two-way repeated-measures ANOVA model was set as ‘dissimilarity - warming + year × block’ using the function *adonis* in the R package *vegan*. Significant effects ($P < 0.05$) are shown in bold text.

over time (Fig. 1d). All these results suggest the convergent succession of the soil archaeal community between warming and control, which is opposite to those observed in bacteria.

The contrasting directions of succession between the domains Archaea and Bacteria in response to experimental warming invalidated our hypothesis of similar succession patterns between the two domains. The opposite directions in succession between soil archaea and bacteria could be due to distinctions in biochemistry, genetics, physiology, ecology and evolution^{42,43}. For instance, the soil archaeal community has relatively low taxonomic and phylogenetic diversity (primarily Nitrososphaerales). These detected archaeal species are also functionally similar with narrow ecological niches (that is, nitrification) and are replacing each other over time, which could result in convergent succession between warming and control. In contrast, the soil bacterial community is taxonomically, phylogenetically and functionally highly diverse. They occupy heterogeneous niches and could be subjected to multiple selection forces (for example, resource limitation and intraspecific competition)⁴² structuring community composition in response to climate warming, which could lead to the more dissimilar community over time.

Effects of warming on archaeal functional structure

The warming-altered archaeal taxonomic and phylogenetic composition could affect functional community structure. To test this, the microbial communities were further analysed using both GeoChip-based functional gene arrays^{34,44} and shotgun metagenomic sequencing. While the shotgun sequencing-based metagenomic approach is ideal for the novel discovery of phylotypes, functional genes, regulators and/or metabolic pathways, the microarray-based detection has advantages for comparative studies in terms of sensitivity, quantitation and reproducibility³⁴. Warming had significant ($P < 0.001$) impacts on the archaeal community functional structure (Adonis analysis, Table 1). Among the 188 archaea-specific genes detected by GeoChip, the abundances of 45 genes (23.9%) significantly decreased under warming (Supplementary Table 3). Some of these significantly impacted genes (16 out of 45 genes) were involved in C and N cycling (Fig. 1e and Supplementary Table 3). Among the 163 archaea-specific genes detected by metagenome EcoFUN-MAP, warming had positive impacts on the abundances of 8 genes and negative impacts on 16 genes, as shown by the response ratios (Supplementary Table 4). Four out of 24 genes significantly altered by warming were involved in C and N cycling (Fig. 1e and Supplementary Table 4). Two genes, *aceB* and *ara*, involved in C cycling were detected by both GeoChip and metagenome EcoFUN-MAP with significant differences between warming and control (Fig. 1e). However, the impacts of warming on these 2 genes as measured by the two methods were opposite. It is most likely that the direction determined by GeoChip (decreased in abundance under warming) reflected the actual impact of warming as the results from *amoA* gene amplicon sequencing agreed with the GeoChip data (Fig. 1e). In addition, 4 genes (*ara*, *cda*, xylanase and *amoA*) from GeoChip but none

from EcoFUN-MAP were strongly correlated with ecosystem C fluxes, including gross primary productivity (GPP) and ecosystem respiration (ER) (Supplementary Tables 5 and 6). The *ara*, *cda* and xylanase genes are involved in C degradation processes and the *amoA* gene in nitrification. Collectively, these results indicate that warming significantly decreased the abundances of certain C and N cycling genes in the soil archaeal community but could strengthen the linkages between the archaeal functional community structure and ecosystem processes.

Community assembly processes in response to warming

To disentangle the community assembly mechanisms involved in the observed temporal succession patterns of the soil archaeal community, we used a phylogenetic bin-based null model analysis (iCAMP)⁴⁵ and found that homogeneous selection (HoS; selection under homogeneous abiotic and biotic conditions in space and time) and drift (DR; random changes in the relative abundances of different species within a community due to the inherent stochastic processes of birth, death and reproduction) dominated archaeal community assembly, with respective relative importance of 14.7% and 84.4% (Fig. 2a). Correspondingly, the partial canonical correlation analysis (CCA)-based variation partitioning analysis indicated that the majority of the community variations (86.4%) could not be explained by the measured soil and plant variables and time (Extended Data Figs. 5 and 6), suggesting that stochastic processes could play dominant roles in the assembly of the soil archaeal community.

Over the years, the archaeal community variation between warming and control showed significant declines in stochasticity (Fig. 2b; slope = -0.015 , $P = 0.016$) and DR (Fig. 2b; slope = -0.016 , $P = 0.028$), but an increase in HoS (Fig. 2b; slope = 0.015 , $P = 0.015$), suggesting a cumulatively enhanced deterministic filtering effect of warming on the soil archaeal community. The increase in warming-induced determinism over time was significantly correlated with total plant biomass and total N (Fig. 2c and Supplementary Table 7; $|R| \geq 0.186$, $P \leq 0.060$). Previous studies reported mixed effects of plant variables (richness and biomass) on deterministic assembly processes of soil bacterial communities^{45,46}, but few reports on those of soil archaeal communities. Soil N content can be a determining factor for the fitness of AOA, the predominant group in soil archaeal communities⁴⁷.

The relative importance of different ecological processes varied substantially among different lineages (bins) (Fig. 3). The members of the predominating order Nitrososphaerales distributed in two bins: Bin2 (containing 23 OTUs and accounting for 83.5% relative abundance) and Bin1 (46 OTUs, 15.1% relative abundance) (Fig. 3a,b). Unexpectedly, these two bins were dominated by different ecological processes—DR for Bin2 (99.8%) and HoS for Bin1 (97.2%). Furthermore, the warming-induced decrease in DR was mainly due to Bin2 (69.1%; Fig. 3c and Extended Data Fig. 7), with OTU1 and OTU2 being the major contributors (contributed 24.3% and 26.1%, respectively; Supplementary Table 8). In contrast, the warming-induced increase in HoS was mainly attributed to the responses of Bin1 (98.6%; Fig. 3d

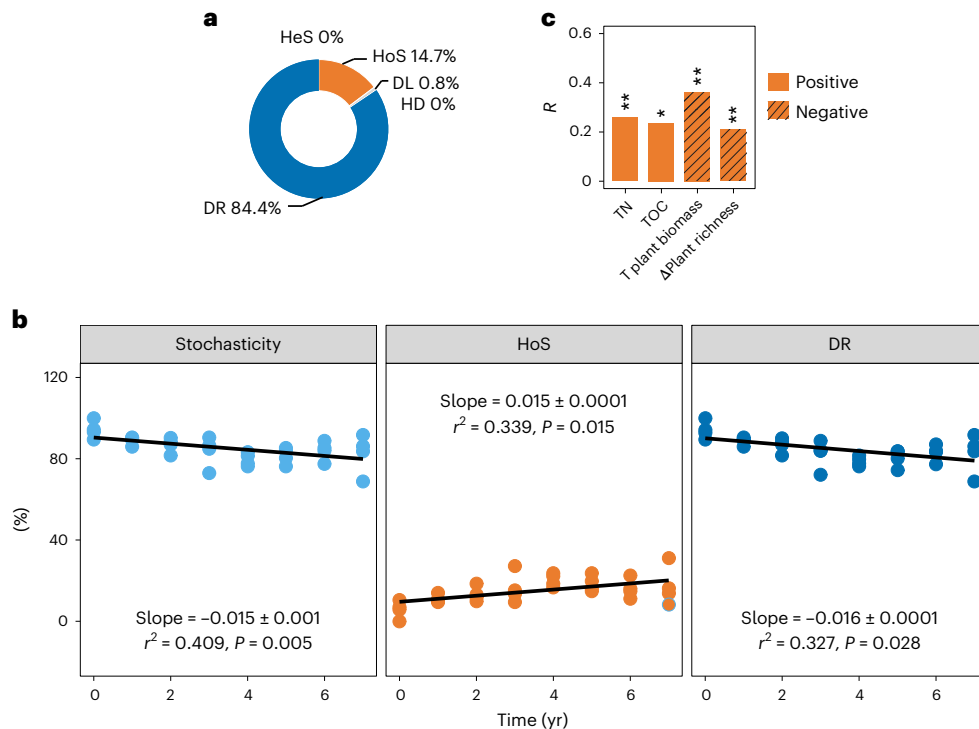


Fig. 2 | Ecological processes and community assembly mechanisms associated with the temporal dynamics in the soil archaeal community.
a, Relative importance of deterministic processes (HoS and HeS) and stochastic processes (DL, HD and DR) between warming and control treatments.
b, Changes in the relative importance of stochastic processes, HoS and DR (%) between warming and control at each block over the years. Results are based on LMMs (statistical tests and significance are the same as in Fig. 1c,d).
c, Effects of environmental factors on deterministic processes defined by the phylogenetic

bin-based null model analysis (iCAMP) based on the Mantel test (two-sided). Only factors with significant correlations are shown ($P = 0.039, 0.062, 0.049, 0.029$ for total N, total organic C, total plant biomass and the difference in plant richness). See Supplementary Table 7 for other factors. R , coefficient of determination from the Mantel analysis. The correlation was determined on the basis of the difference (with a triangle before the name) or the mean (without a triangle) of a factor between each pair of samples. ** $P < 0.05$; * $P < 0.10$.

and Extended Data Fig. 7), with OTU3 and OTU11 being the top contributors (contributed 33.6% and 20.3%, respectively; Supplementary Table 8). Altogether, these results demonstrated complex assembly mechanisms of different taxa in response to warming, even within Nitrososphaerales.

Links between archaeal community structure and functioning

We compared correlations between archaeal community structure and environmental variables and ecosystem functioning under control and warming (Fig. 4a and Extended Data Fig. 8). The archaeal community measured by both taxonomic and gene functional compositions generally exhibited stronger correlations with various environmental variables and ecosystem functioning under warming than in the control (Fig. 4a and Extended Data Fig. 8). In fact, $\text{NH}_4^+\text{-N}$, C_3 plant biomass, ER and GPP were significantly correlated with archaeal community structure under warming (Fig. 4a and Extended Data Fig. 8; $P < 0.05$). Year was the most influential factor affecting archaeal community taxonomic and functional compositions under both warming and control, followed by total plant biomass. In addition, soil pH, precipitation of the sampling month, drought index, soil moisture and ecosystem C fluxes, including net ecosystem exchange (NEE) and heterotrophic soil respiration (R_h), were also factors significantly associated with archaeal community structure shared under warming and control (Fig. 4a and Extended Data Fig. 8; $P < 0.05$). Nevertheless, only a limited number of examined variables showed significant correlations with archaeal community taxonomic and functional structures under both warming and control.

Partial least squares (PLS) analysis was further used to understand the environmental drivers of archaeal community diversity, succession and associated functions under warming treatment (Fig. 4b and Supplementary Table 9). Warming had a strong positive influence on soil temperature (Pearson correlation $r = 0.92$, partial $R^2 = 0.38$, $P = 0.044$) and to a lesser extent on soil pH ($r = 0.003$, partial $R^2 = 0.17$, $P = 0.015$), but a negative influence on soil moisture ($r = -0.50$, partial $R^2 = 0.22$, $P = 0.007$). Warming decreased archaeal community richness ($r = -0.52$, partial $R^2 = 0.21$, $P = 0.016$), archaeal C degradation gene abundances ($r = -0.57$, partial $R^2 = 0.25$, $P = 0.002$) and N functional gene abundances ($r = -0.62$, partial $R^2 = 0.20$, $P = 0.001$). In addition, warming could shape archaeal community structure (that is, β -diversity, PC2) indirectly through soil temperature ($r = -0.03$, partial $R^2 = 0.23$, $P = 0.036$) and archaeal community richness ($r = -0.94$, partial $R^2 = 0.45$, $P = 0.005$). Soil total N (partial $R^2 \geq 0.24$, $P \leq 0.005$) and archaeal functional traits (that is, nitrification and denitrification; partial $R^2 \geq 0.20$, $P \leq 0.011$) also had strong effects on archaeal β -diversity. Furthermore, the archaeal community functional traits involved in methane and denitrification could positively impact ecosystem functions by affecting ER (partial $R^2 \geq 0.17$, $P \leq 0.006$). Lastly, the PLS model showed that soil properties such as soil total organic C, soil $\text{NH}_4^+\text{-N}$, soil moisture and soil temperature could directly shape ecosystem functions, including autotrophic respiration (R_a), R_h , NEE and ER (partial $R^2 \geq 0.34$, $P \leq 0.006$). Together, these results indicated that experimental warming could shape the soil archaeal community directly or indirectly through soil temperature and that soil archaeal community structure was crucial in mediating changes in ecosystem functioning.

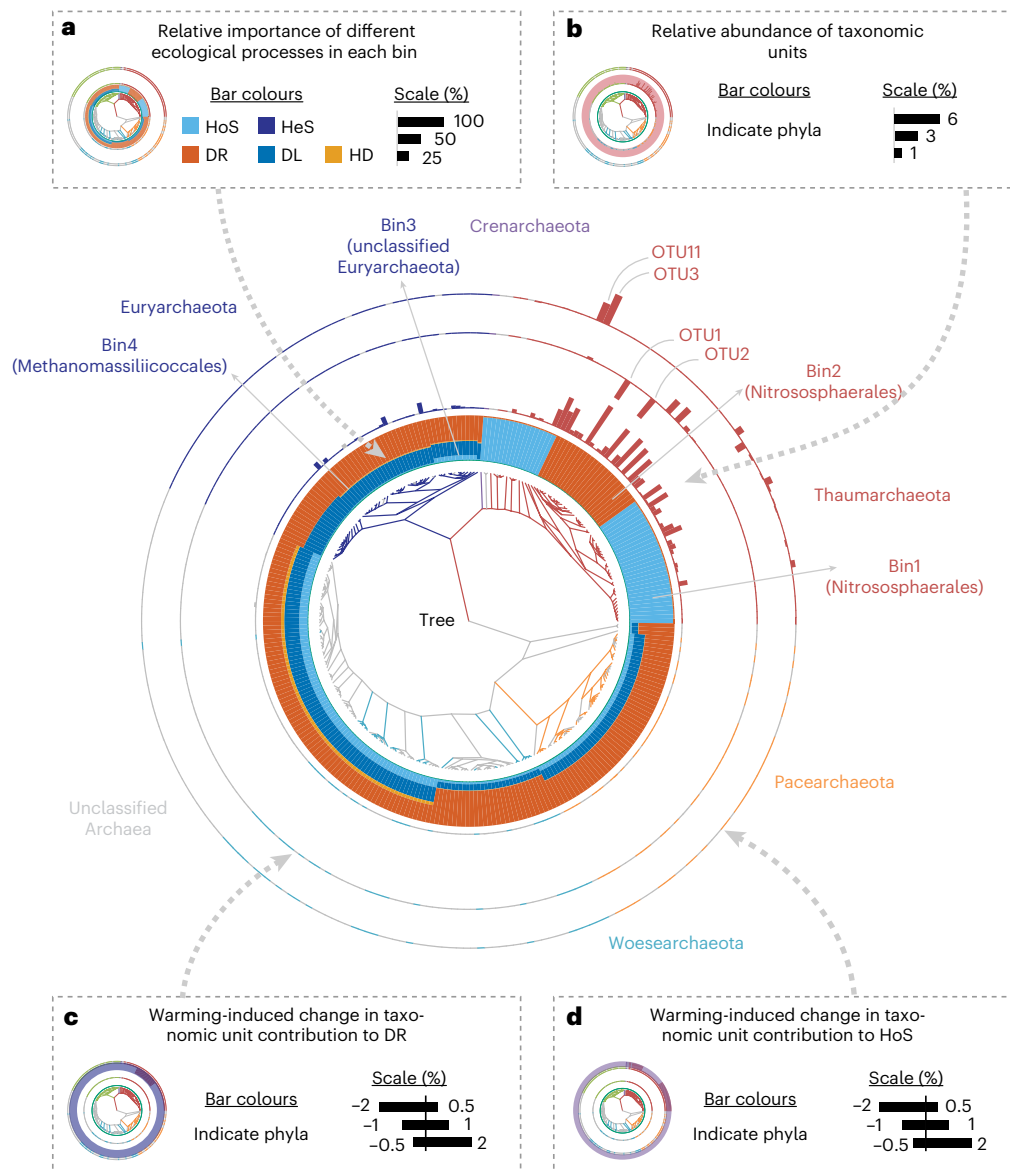


Fig. 3 | Variations of ecological processes across different phylogenetic groups. The phylogenetic tree is displayed at the centre. **a**, Relative importance of different ecological processes in each bin (stacked bars in the first annulus). **b**, Relative abundance of individual taxonomic units (second annulus). All 287 taxonomic units are shown. **c**, Warming-induced change in taxonomic unit contribution to drift (third annulus) and **d**, homogeneous selection

(fourth annulus), where positive (outward bar) and negative (inward bar) represent increase and decrease by warming, respectively. The most abundant bins are marked in the figure, including Bin2 (83.5% relative abundance; dominated by Nitrososphaerales), Bin1 (15.1%; Nitrososphaerales), Bin4 (0.9%; Methanomassiliicoccales) and Bin3 (0.2%; unclassified Euryarchaeota).

Concluding remarks

Understanding temporal dynamics and its underlying mechanisms within the context of climate change is a fundamental issue in ecology; however, very few studies have examined the impacts of climate warming on Archaea. This study provides several important insights into the responses of the archaeal community to climate warming. First, consistent with our recent findings on soil bacteria, fungi and protists²⁷, we demonstrate that climate warming reduced the taxonomic, phylogenetic and possibly functional diversity of soil archaeal community, which provides explicit evidence supporting microbial biodiversity loss under long-term climate warming in a field setting. Second, in contrast to soil bacteria and fungi²⁵, we reveal that warming played an important role in accelerating the temporal succession of the soil archaeal community towards higher convergence, which could primarily be due to their distinct differences in biochemistry, physiology, ecology and

evolution⁸. In addition, our results demonstrate that the succession of the soil archaeal community to the perturbations of climate warming was primarily controlled by stochastic processes, and experimental warming, acting as a filtering factor, reduced stochasticity.

Our findings have important implications for understanding and predicting the ecological consequences of climate change. Because stochasticity reduces under warming as time proceeds, the communities can converge more quickly to a community state with less stochasticity under warming. As a result, the archaeal community composition and structure might be less variable and more predictable under future climate warming. Also, since soil archaeal biodiversity decreases under warming, the future ecosystems in a warmer world will be less diverse. It is expected that the linked ecosystem functions and services could become more vulnerable under future climate warming scenarios³⁸. Consequently, the detrimental effects of biodiversity loss could be

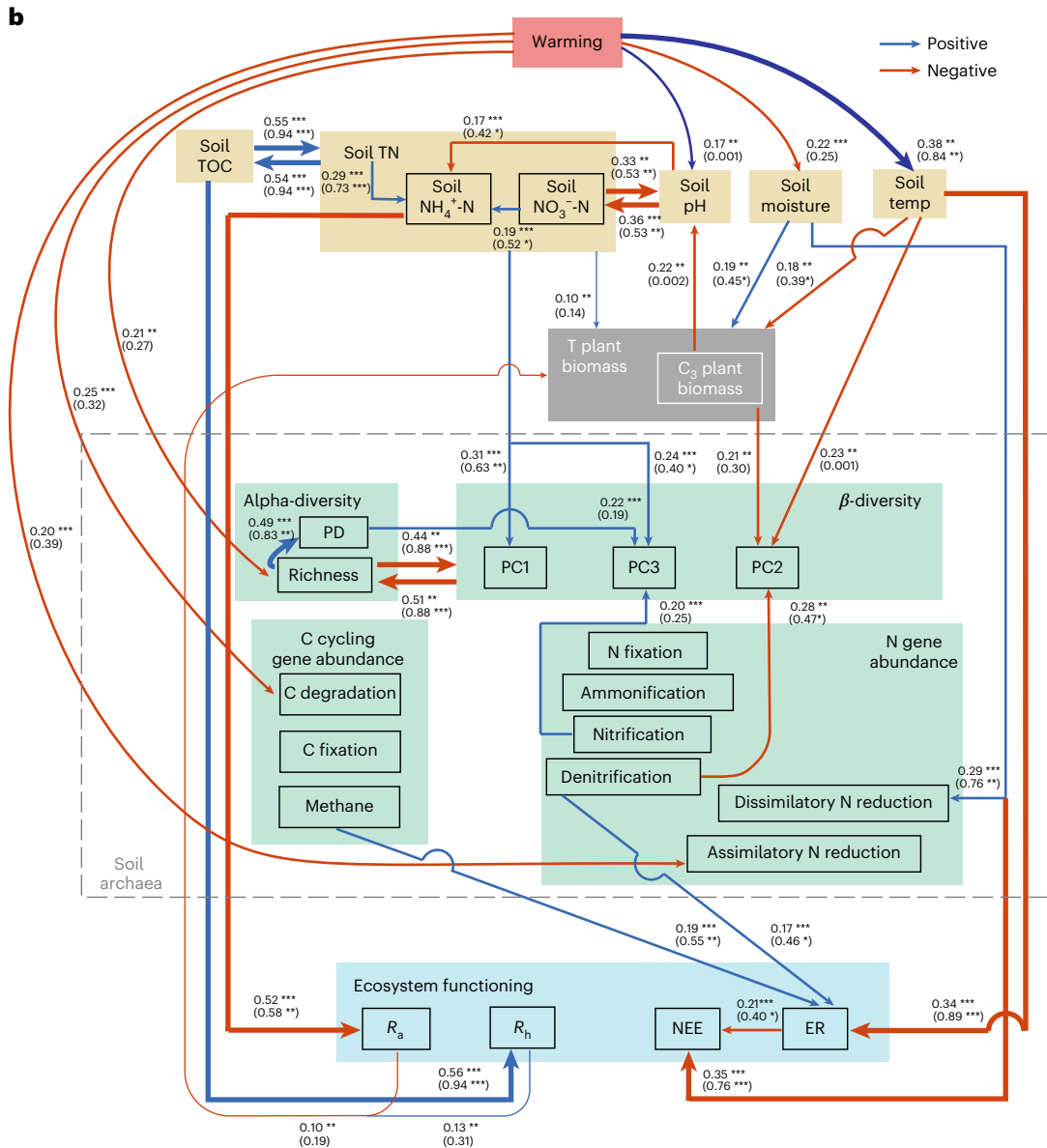
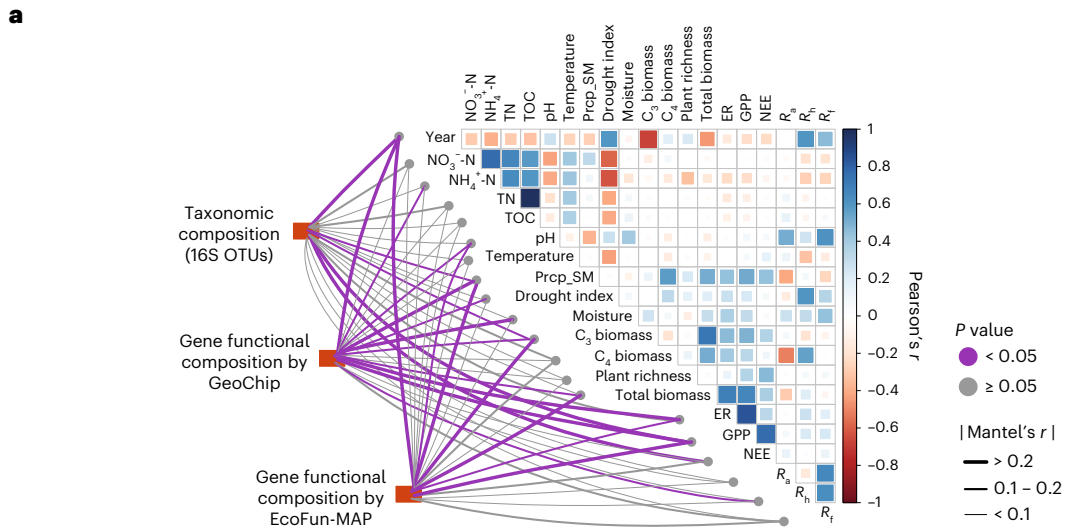


Fig. 4 | Environmental drivers of archaeal community structure and functioning. **a**, Relationships between archaeal community structure and environmental variables and ecosystem processes under warming. See Extended Data Fig. 8 for under control conditions. Archaeal community structures, which include taxonomic composition by 16S rRNA genes and functional gene composition by GeoChip and EcoFUN-MAP, were tested against time, soil and plant variables, and ecosystem C fluxes. The edge width corresponds to Mantel's r value, and the edge colour denotes statistical significance (two-sided). Pairwise correlations of these variables are shown with a colour gradient denoting Pearson's correlation coefficient. Soil variables include soil nitrate (NO_3^-), ammonium (NH_4^+), total nitrogen (TN), total organic C (TOC), pH, precipitation of the sampling month (Prcp_SM), temperature, moisture and drought index; plant variables include C_3 and C_4 aboveground biomass, plant richness and total biomass; ecosystem C fluxes include ER, GPP, NEE, R_g , R_h and R_t . **b**, PLS models of

the relationships among treatments (warming), soil properties, plant variables, archaeal community diversity and functional traits and ecosystem functions. Directions for all arrows are from independent variable(s) to a dependent variable in the forward selected PLS models ($P < 0.05$ for both R^2 , and Q^2 ; two-sided); only the most relevant variables (variable influence on projection > 1) are presented. The numbers near the pathway arrow indicate the proportion of variance explained for every dependent variable, with the top row representing the partial R^2 index based on PLS (see details in Methods) and the bottom row representing Pearson correlation R^2 . The asterisks denote the significance levels of each optimum PLS model (top row) and Pearson correlation (bottom row). *** $P < 0.01$, ** $P < 0.05$ and * $P < 0.10$. The grey dashed box indicates parameters for the soil archaeal community. The widths of pathways are proportional to the partial R^2 index.

more severe. However, further research is needed to examine whether the warming-induced convergent succession, archaeal biodiversity loss and associated mechanisms are applicable to other ecosystems.

Online content

Any methods, additional references, Nature Portfolio reporting summaries, source data, extended data, supplementary information, acknowledgements, peer review information; details of author contributions and competing interests; and statements of data and code availability are available at <https://doi.org/10.1038/s41558-023-01664-x>.

References

- Woese, C. R., Kandler, O. & Wheelis, M. L. Towards a natural system of organisms: proposal for the domains Archaea, Bacteria, and Eucarya. *Proc. Natl Acad. Sci. USA* **87**, 4576–4579 (1990).
- Hedlund, B. P., Zhang, C., Wang, F., Rinke, C. & Martin, W. F. Editorial: ecology, metabolism and evolution of archaea—perspectives from Proceedings of the International Workshop on Geo-Omics of Archaea. *Front. Microbiol.* **12**, 827229 (2021).
- DeLong, E. F. Archaea in coastal marine environments. *Proc. Natl Acad. Sci. USA* **89**, 5685–5689 (1992).
- Fuhrman, J. A., McCallum, K. & Davis, A. A. Novel major archaeobacterial group from marine plankton. *Nature* **356**, 148–149 (1992).
- DeLong, E. F. Exploring marine planktonic archaea: then and now. *Front. Microbiol.* **11**, 616086 (2021).
- Karimi, B. et al. Biogeography of soil bacteria and archaea across France. *Sci. Adv.* **4**, eaat1808 (2018).
- Tahon, G., Geesink, P. & Ettema, T. J. G. Expanding archaeal diversity and phylogeny: past, present, and future. *Annu. Rev. Microbiol.* **75**, 359–381 (2021).
- Baker, B. J. et al. Diversity, ecology and evolution of Archaea. *Nat. Microbiol.* **5**, 887–900 (2020).
- Needham, D. M. & Fuhrman, J. A. Pronounced daily succession of phytoplankton, archaea and bacteria following a spring bloom. *Nat. Microbiol.* **1**, 16005 (2016).
- Shu, W. S. & Huang, L. N. Microbial diversity in extreme environments. *Nat. Rev. Microbiol.* **20**, 219–235 (2021).
- Adam, P. S., Borrel, G., Brochier-Armanet, C. & Gribaldo, S. The growing tree of Archaea: new perspectives on their diversity, evolution and ecology. *ISME J.* **11**, 2407–2425 (2017).
- Zaremba-Niedzwiedzka, K. et al. Asgard archaea illuminate the origin of eukaryotic cellular complexity. *Nature* **541**, 353–358 (2017).
- Imachi, H. et al. Isolation of an archaeon at the prokaryote-eukaryote interface. *Nature* **577**, 519–525 (2020).
- Liu, Y. et al. Expanded diversity of Asgard archaea and their relationships with eukaryotes. *Nature* **593**, 553–557 (2021).
- Angel, R., Soares, M. I., Ungar, E. D. & Gillor, O. Biogeography of soil archaea and bacteria along a steep precipitation gradient. *ISME J.* **4**, 553–563 (2010).
- Auguet, J. C., Barberan, A. & Casamayor, E. O. Global ecological patterns in uncultured Archaea. *ISME J.* **4**, 182–190 (2010).
- Bates, S. T. et al. Examining the global distribution of dominant archaeal populations in soil. *ISME J.* **5**, 908–917 (2011).
- Bar-On, Y. M., Phillips, R. & Milo, R. The biomass distribution on Earth. *Proc. Natl Acad. Sci. USA* **115**, 6506–6511 (2018).
- Offre, P., Spang, A. & Schleper, C. Archaea in biogeochemical cycles. *Annu. Rev. Microbiol.* **67**, 437–457 (2013).
- Leininger, S. et al. Archaea predominate among ammonia-oxidizing prokaryotes in soils. *Nature* **442**, 806–809 (2006).
- Danovaro, R., Rastelli, E., Corinaldesi, C., Tangherlini, M. & Dell'Anno, A. Marine archaea and archaeal viruses under global change. *F1000Research* **6**, 1241 (2017).
- Goberna, M., Garcia, C., Insam, H., Hernandez, M. T. & Verdu, M. Burning fire-prone Mediterranean shrublands: immediate changes in soil microbial community structure and ecosystem functions. *Microb. Ecol.* **64**, 242–255 (2012).
- Gschwendtner, S. et al. Climate change induces shifts in abundance and activity pattern of bacteria and archaea catalyzing major transformation steps in nitrogen turnover in a soil from a mid-European beech forest. *PLoS ONE* **9**, e114278 (2014).
- Hayden, H. L. et al. Changes in the microbial community structure of bacteria, archaea and fungi in response to elevated CO_2 and warming in an Australian native grassland soil. *Environ. Microbiol.* **14**, 3081–3096 (2012).
- Guo, X. et al. Climate warming leads to divergent succession of grassland microbial communities. *Nat. Clim. Change* **8**, 813–818 (2018).
- Guo, X. et al. Climate warming accelerates temporal scaling of grassland soil microbial biodiversity. *Nat. Ecol. Evol.* **3**, 612–619 (2019).
- Wu, L. et al. Reduction of microbial diversity in grassland soil is driven by long-term climate warming. *Nat. Microbiol.* **7**, 1054–1062 (2022).
- Yuan, M. M. et al. Climate warming enhances microbial network complexity and stability. *Nat. Clim. Change* **11**, 343–348 (2021).
- Cavicchioli, R. Archaea—timeline of the third domain. *Nat. Rev. Microbiol.* **9**, 51–61 (2011).
- Prach, K. & Walker, L. R. Four opportunities for studies of ecological succession. *Trends Ecol. Evol.* **26**, 119–123 (2011).
- Xu, X., Sherry, R. A., Niu, S. L., Li, D. J. & Luo, Y. Q. Net primary productivity and rain-use efficiency as affected by warming, altered precipitation, and clipping in a mixed-grass prairie. *Glob. Change Biol.* **19**, 2753–2764 (2013).

32. Kerou, M., Alves, R. J. E. & Schleper, C. in *Bergey's Manual of Systematics of Archaea and Bacteria* (eds Trujillo, M. E. et al.) <https://doi.org/10.1002/9781118960608.obm00124> (John Wiley & Sons, 2018).
33. Nkamga, V. D. & Drancourt, M. in *Bergey's Manual of Systematics of Archaea and Bacteria* (eds Trujillo, M. E. et al.) <https://doi.org/10.1002/9781118960608.gbm01365> (John Wiley & Sons, 2016).
34. Zhou, J. et al. High-throughput metagenomic technologies for complex microbial community analysis: open and closed formats. *mBio* **6**, e02288-14 (2015).
35. Zhou, J. et al. Random sampling process leads to overestimation of beta-diversity of microbial communities. *mBio* **4**, e00324-13 (2013).
36. Xue, K. et al. Tundra soil carbon is vulnerable to rapid microbial decomposition under climate warming. *Nat. Clim. Change* **6**, 595–600 (2016).
37. Pecl, G. T. et al. Biodiversity redistribution under climate change: impacts on ecosystems and human well-being. *Science* **355**, eaai9214 (2017).
38. Cardinale, B. J. et al. Biodiversity loss and its impact on humanity. *Nature* **486**, 59–67 (2012).
39. Li, D., Miller, J. E. D. & Harrison, S. Climate drives loss of phylogenetic diversity in a grassland community. *Proc. Natl Acad. Sci. USA* **116**, 19989–19994 (2019).
40. Fei, S. et al. Divergence of species responses to climate change. *Sci. Adv.* **3**, e1603055 (2017).
41. Bascompte, J., García, M. B., Ortega, R., Rezende, E. L. & Pironon, S. Mutualistic interactions reshuffle the effects of climate change on plants across the tree of life. *Sci. Adv.* **5**, eaav2539 (2019).
42. Kerou, M. et al. Proteomics and comparative genomics of *Nitrososphaera viennensis* reveal the core genome and adaptations of archaeal ammonia oxidizers. *Proc. Natl Acad. Sci. USA* **113**, E7937–E7946 (2016).
43. Taylor, A. E., Giguere, A. T., Zobelein, C. M., Myrold, D. D. & Bottomley, P. J. Modeling of soil nitrification responses to temperature reveals thermodynamic differences between ammonia-oxidizing activity of archaea and bacteria. *ISME J.* **11**, 896–908 (2017).
44. Shi, Z. et al. Functional gene array-based ultrasensitive and quantitative detection of microbial populations in complex communities. *mSystems* **4**, e00296-19 (2019).
45. Ning, D. L. et al. A quantitative framework reveals ecological drivers of grassland microbial community assembly in response to warming. *Nat. Commun.* **11**, 4717 (2020).
46. Liu, L. et al. Changes in assembly processes of soil microbial communities during secondary succession in two subtropical forests. *Soil Biol. Biochem.* **154**, 108144 (2021).
47. Verhamme, D. T., Prosser, J. I. & Nicol, G. W. Ammonia concentration determines differential growth of ammonia-oxidizing archaea and bacteria in soil microcosms. *ISME J.* **5**, 1067–1071 (2011).

Publisher's note Springer Nature remains neutral with regard to jurisdictional claims in published maps and institutional affiliations.

Springer Nature or its licensor (e.g. a society or other partner) holds exclusive rights to this article under a publishing agreement with the author(s) or other rightsholder(s); author self-archiving of the accepted manuscript version of this article is solely governed by the terms of such publishing agreement and applicable law.

© The Author(s), under exclusive licence to Springer Nature Limited 2023

Methods

Site description

The study site was located at the Kessler Atmospheric and Ecological Field Station (KAEFS) in the US Great Plains in McClain County, Oklahoma (34° 59' N, 97° 31' W)³¹. The design of this site has been previously described in detail^{25,28,48}. Briefly, KAEFS is a temperate grassland with an average air temperature of 16.3 °C and an average annual precipitation of 914 mm (data from the Oklahoma Climatological Survey from 1948 to 1999). The experimental site was dominated by C₃ forbs (*Solanum carolinense*, *Ambrosia trifida* and *Euphorbia dentata*), C₃ grasses (*Bromus* spp.) and C₄ grasses (*Tridens flavus* and *Sorghum halapense*). The soil type was Port-Pulaski-Keokuk complex with a neutral pH, a high available water holding capacity (37%) and a deep (-70 cm) moderately penetrable root zone²⁵. The concentrations of soil organic matter and total N are 1.9% and 0.1%, respectively, and the soil bulk density is 1.2 g cm⁻³.

The field experiment started in July 2009 and is a split-block design, with warming (+3 °C) as the primary factor. Two levels of warming (ambient and +3 °C) were set for four pairs of 2.5 m × 1.75 m plots by utilizing a 'real' infrared radiator (Kalglo Electronics) for warmed plots or a 'dummy' infrared radiator (Kalglo Electronics) for the corresponding control plots to account for the shading effects. In this study, data generated from this site between 2009 and 2016 were used.

Field measurements

Soil temperature was monitored using constantan-copper thermocouples every 15 min at 7.5, 20, 45 and 75 cm in the centre of each plot. We used the annual average values at 7.5 cm depth across the whole year to represent the microclimate of the surface soil sampled (0–15 cm). Soil moisture, expressed as volumetric soil water content (%v), was measured once or twice a month using a portable time domain reflectometer (Soil Moisture Equipment) from the soil surface to a depth of 15 cm. The average values of three measurements in each plot were used as monthly averages and the average of soil moisture data across each year is presented in this study. All species within each plot were identified to estimate species richness. Aboveground plant biomass was estimated by a modified pin-touch method^{31,49}, with C₃ and C₄ species separated⁵⁰.

Ecosystem C fluxes, including NEE, ER, GPP, soil total respiration (R_t), R_h and R_a were measured once or twice a month between 10:00 and 15:00 (local time)^{31,51}. NEE and ER were measured using an LI-6400 portable photosynthesis system (LI-COR) attached to a transparent chamber (0.5 m × 0.5 m × 0.7 m). R_t and R_h were measured using an LI-8100A soil flux system attached to a soil CO₂ flux chamber (LI-COR)⁵². GPP was estimated as the difference between NEE and ER, and R_a was the difference between R_t and R_h . The average values of ecosystem C flux and respiration across each year were used in this study.

Sampling

We collected 8 surface (0–15 cm) soil samples annually in 4 control and 4 warmed plots from 2010 to 2016 (Y1–Y7) during the peak plant biomass season (September to October). Eight pre-warmed samples were taken in 2009 (Y0). Each soil sample was a mixture of 3 soil cores (2.5 cm diameter × 15 cm depth) taken with a soil sampler tube to reduce variation caused by soil heterogeneity. A total of 64 soil samples from 4 replicate plots under warming and control (ambient) conditions were included and analysed in this study. Soil samples were kept on ice for less than 2 h before they were transferred to the laboratory located at the University of Oklahoma.

Soil chemistry

After removing visible roots (>0.25 cm) and rocks, soil samples were sent to the Soil, Water and Forage Analytical Laboratory at the Oklahoma State University for chemical analyses, including organic C and total N contents, soil nitrate (NO₃⁻) and ammonium (NH₄⁺) and soil pH. Detailed information could be found in our previous publication²⁵.

As shown previously, experimental warming significantly altered aboveground plants, ecosystem processes and soil conditions^{25,48}. For microbiological analyses, samples were stored at -80 °C before DNA extraction.

DNA extraction

Soil DNA was extracted from 1.5 g of each well-mixed soil sample using a previously published protocol^{25,53}, including freeze-grinding treatment, SDS-based lysis and purification with a MoBio PowerSoil DNA isolation kit (MoBio Laboratories). DNA quality was assessed with a NanoDrop ND-1000 spectrophotometer (Thermo Fisher) and a ratio of 2.0–2.2 for optical density (OD)₂₆₀/OD₂₃₀ and 1.7–2.0 for OD₂₆₀/OD₂₈₀ indicated good quality. The final DNA concentrations were quantified by PicoGreen using a FLUOstar Optima fluorescence plant reader (BMG Labtech). DNAs were stored at -80 °C before sequencing analysis²⁵.

Amplicon sequencing

We used a two-step PCR amplification protocol for constructing the sequencing library to reduce sequencing errors, minimize amplification bias and preserve semi-quantitative information of PCR amplification^{36,54,55}. In this study, we used one primer set targeting the V3–V4 hypervariable region of the archaeal 16S rRNA genes: 519F (5' - CAGYMGCCRCGGKAAHACC -3') and 806R (5' - GGACTACNSGGTMTCTAAT -3')^{56–58}. To amplify the archaeal *amoA* genes, the primer set: 5' - STAATGGTCTGGCTTAGACG -3' and 5' - GCGGCATCCATCTGTATGT -3' (ref. 59) was used. In addition, the primer set: 515F (5' - GTGCCAGCMGCCGCGGTAA -3') and 806R (5' - GGACTACHVGGGTWCTAAT -3') was used for bacterial community profiling⁶⁰. During the first amplification step, 10 ng DNA from each sample was PCR-amplified for 10 cycles in a 25 µl reaction volume with the primers without adaptors. The obtained PCR products were then purified and dissolved in 50 µl deionized water. During the second amplification step, 15 µl of the PCR products from each sample were amplified using the primers with adaptors, barcodes and spacers for an additional 15 cycles. The PCR reactions at each step were done in triplicates. Paired-end sequencing of the amplicons (2 × 250 bp) was done with an Illumina MiSeq platform following manufacturer instructions for both the archaeal and bacterial 16S rRNA genes^{54,55}. For sequencing the archaeal *amoA* gene amplicons, MiSeq reagent kit v3 (2 × 300 bp) (Illumina) was used. An average of 29,900 ± 20,800, 25,296 ± 20,560 and 59,900 ± 36,700 sequence reads per sample were obtained for the archaeal 16S rRNA genes, archaeal *amoA* genes and bacterial 16S rRNA genes, respectively.

Sequence preprocessing

The raw reads of sequences were analysed using a sequence analysis pipeline built on the Galaxy platform (v0.1.0), developed by the Institute for Environmental Genomics⁶¹ (<http://zhoulab5.rccc.ou.edu:8080>). Primer sequences were trimmed from the paired-end sequences and filtered by the Btrim programme⁶² with a quality score threshold of 20 over a 5 bp window size. Forward and reverse reads of the same sequence with at least 20 bp overlap and <5% mismatches were combined using FLASH⁶³. Any joined sequences with an ambiguous base or a length of <245 bp were discarded. Because the expected lengths of the archaeal *amoA* gene amplicons (635 bp) were larger than the summed length of forward and reverse reads (600 bp), we only used the forward reads of the archaeal *amoA* gene amplicons with a cut-off length of 273 nt. Thereafter, OTUs were clustered by UPARSE⁶⁴ at 97% identity and singletons were removed from the remaining sequences^{64,65}. The Greengenes reference dataset⁶⁶ for 16S data was used as a reference database to remove chimaeras. For the archaeal community, each sample was rarefied to a sequencing depth of 7,860 to achieve the same total read abundance. A total of 287 OTUs (at 97% similarity) were obtained across all samples. Rarefaction curves approached saturation, suggesting that this level of sequencing effort

was sufficient to estimate the diversity of the soil archaeal community (Supplementary Fig. 1). In comparison, the bacterial community was rarefied to a sequencing depth of 21,200, with 35,306 OTUs across all samples. OTU taxonomic classification was performed using representative sequences from each OTU through the Ribosomal Database Project Classifier with 50% confidence estimates⁶⁷. We also constructed community profiling on the basis of amplicon sequence variants (ASVs) using three widely used denoising packages: UNOISE3 (ref. 68), DADA2 (ref. 69) and Deblur⁷⁰. We compared the effects of experimental warming on the resulting community profiles using three non-parametric multivariate statistical tests (Adonis, ANOSIM and MRPP; Supplementary Table 2). OTU-based archaeal community structure was significantly altered by the 7 yr warming treatment in all three statistical tests ($P < 0.050$), while UNOISE3, DADA2 and Deblur community profiles showed significant ($P < 0.050$) or marginally significant ($P < 0.100$) differences with warming treatment in some of the tests but not all (Supplementary Table 1). This suggested that the community structure obtained from OTU-based clustering was more robust to different statistical tests and agreed with the experimental setup. Therefore, the community profiling obtained from OTU-based clustering was used in the subsequent analyses.

Diversity analyses

Richness and Faith's index were used to measure taxonomic and phylogenetic α -diversity, respectively, and they were computed using the Picante R package⁷¹. To estimate phylogenetic β -diversity, the representative amplicon sequences were aligned using Clustal Omega v1.2.2 (ref. 72) for constructing the phylogenetic tree by FastTree2 v2.1.10 (ref. 73). The FastTree topology search was constrained with the relatively reliable 16S-based phylogenetic tree in Silva Living Tree Project⁷⁴ release 132. Unweighted UniFrac distances and Sorensen dissimilarity metrics were calculated to estimate β -diversity on the basis of the resampled OTU tables in R using the vegan package⁷⁵.

Measurement of community turnover

The impacts of warming on the temporal change in the archaeal and bacterial community structure were measured by the distances of microbial communities between warming and control at each block in each year⁷⁶. As we had four replicates (one replicate within each block) for both warming and control treatments, four pairwise comparisons were obtained each year. In this way, the difference between each pair of plots (D) was not subject to (in theory) the effects of experimental noise (due to annual sampling time differences, environmental fluctuations, molecular marker resolution and/or technical variation) on community temporal turnovers. We then fitted the temporal change to the LMM with a random intercept and slope effect among different pairs of plots (blocks)²⁵, $D - t + (1 + t)|\text{Block}$. In this model, D represents dissimilarity between warming and control, and t represents year. The slope of the model is the rate of temporal change in community structure between warming and control, which is a measure of community turnover. The coefficient of determination (R^2) was calculated for each LMM as described previously (named conditional R^2 in ref. 77). The significance of each LMM was calculated by a permutation test, the eight time points (years) randomized for >40,000 times (complete enumeration), and the P value calculated by comparing the Akaike information criterion of the observed LMM with the permuted ones. We also performed a permutation test to calculate the significance of the difference in slopes between warming and control⁷⁸. The P value was generated by comparing the observed slope difference between warming and control with the difference in the permuted datasets²⁵.

Functional profiling

GeoChip 5.0M, a functional gene array³⁴, was used for functional profiling of the 64 samples from 2009 to 2016. GeoChip hybridization,

scanning and data processing were performed at the Institute for Environmental Genomics, the University of Oklahoma, following an established protocol^{34,44}.

The slides hybridized with genomic DNA were imaged as a Multi-TIFF with a NimbleGen MS200 microarray scanner (Roche NimbleGen). The raw signals from NimbleGen were submitted to the Microarray Data Manager (<http://ieg.ou.edu/microarray>), cleaned, normalized and analysed using the data analysis pipeline. First, probes with poor or low signals were removed using a cut-off for the coefficient of variance (CV; probe signal SD/signal) >0.8. Then, the signal-to-noise ratio was calculated with the average signal of Agilent's negative control probes within each subarray. The signal intensity for each spot was corrected by subtracting the background signal intensity. If the net difference was <0, the spots were excluded from subsequent analysis⁴⁴. To normalize signal intensities, the sum of the signal intensity was calculated for each array, and the maximum sum value was used to normalize the signal intensity of all spots in each array. We extracted 2,524 archaea-specific probes from the entire dataset on the basis of their lineage information, these probes belonging to 188 archaea-specific genes. All analyses were done using the extracted subset of data.

Metagenomics of individual samples from 2009 to 2016 was also used for functional profiling. Metagenomic libraries were prepared using a KAPA Hyper Prep kit (KR0961) following manufacturer instructions and sequenced at the Oklahoma Medical Research Foundation's Genomics Core using the Illumina HiSeq 3000 platform with a 2×150 bp paired-end kit. We obtained 1,100.14 gigabases (Gb) of data in total, with an average of 17.19 ± 2.68 Gb per sample²⁷. Processing of the metagenomic sequences included quality evaluation by FastQC⁷⁹, duplicate removal by CD-HIT⁸⁰ with an identity cut-off of 100% and quality filtering by NGS QC Toolkit (v2.3.3)⁸¹. Bases with a quality score <20 were trimmed from the 3' end until the first base had a quality score ≥ 20 . Trimmed reads with a length of >120 and an average quality score ≥ 20 were kept. In addition, reads with more than one ambiguous base were removed²⁷. All reads were submitted to our EcoFUN-MAP pipeline (<http://www.ou.edu/ieg/tools/dataanalysis-pipeline.html>) to extract shotgun sequence reads of environmental importance³⁶. Archaea-specific gene clusters were extracted from the entire dataset on the basis of their lineage information, resulting in 21,031 gene clusters belonging to 163 genes. This archaea-specific dataset was used in the subsequent analyses.

Community assembly

The iCAMP framework was used to investigate the community assembly mechanisms at the level of individual taxa/lineages⁴⁵. The R code for iCAMP is available as an open-source R package, iCAMP and a web-based pipeline (<http://ieg3.rccc.ou.edu:8080>) built on the Galaxy platform (v18.09)⁶¹. iCAMP could differentiate the relative importance of five assembly processes to both the whole community and individual taxa/lineages, including HoS, heterogeneous selection (HeS), dispersal limitation (DL), homogenizing dispersal (HD), and drift and others (DR)^{45,82}. Defined in iCAMP, HoS and HeS constituted deterministic processes, while DL, HD and DR constituted stochastic processes. Our analyses were based on a phylogenetic distance threshold for the significant phylogenetic signal of 0.2 and a minimal bin size of 12. Detailed explanations of the settings for individual parameters could be found in a previous study⁴⁵. The five assembly processes were assessed for their relative importance in governing community variations between warmed plots and control plots. Then, the relative importance of each process was fitted to an LMM with a random intercept and slope effect among different pairs of plots (blocks). The model was set as $M - t + (1 + t)|\text{Block}$, where M represents the relative importance (%) of a process and t represents year. The coefficient of determination (R^2) and the significance of each LMM were determined as described above.

Statistical analyses

Statistical analyses were carried out using R software 4.0.2 with the package *vegan* (v.2.5-7) unless otherwise indicated. Three different non-parametric multivariate statistical tests (Adonis, ANOSIM and MRPP) were used to test the differences in soil microbial communities under warming and control treatments⁵¹. For Adonis, the one-way repeated-measures analysis of variance (ANOVA) model was set as ‘dissimilarity - warming + block × year’ when using the function *Adonis* in the R package *vegan*. For ANOSIM and MRPP, the permutation was constrained within each block in each year by setting ‘strata’ in the functions *ANOSIM* and *MRPP* in the R package *vegan*²⁵. CCA was performed to determine the linkage between ecosystem functional parameters and microbial community structures. The significance of the CCA model was tested using ANOVA. On the basis of the CCA results, variation partitioning analysis was performed to determine the contributions of each variable or group of variables to total variations in the soil microbial community composition. Mantel and partial Mantel tests were also performed to calculate the correlations between environmental factors and soil microbial communities.

The PLS model was used to explore the relationships among treatments (warming), archaea community diversity, plant variables and soil properties⁸³. Each optimum PLS model was forward selected from all factors that might affect the dependent variable in biology/biogeochemistry, on the basis of predictive performance counting in the explained variation (R^2) and model significance (P for R^2_Y and $Q^2_Y < 0.05$, where significant Q^2_Y helps to avoid overfitting). To visualize relevant associations, we only included the most relevant variable(s) with variable influence on projection (VIP) values higher than 1.00 (ref. 83). When used as independent variables in PLS, the archaeal community β -diversity was represented by the PCI-3 from principal coordinates analysis of Sorensen distance. Inspired by VIP, we proposed a partial R^2 index on the basis of PLS to represent the proportion of variance explained by each independent variable (equation 1). As a reference, we also calculated the pairwise correlation coefficient (as well as the R^2) among the factors and the significance was based on Pearson correlation (between vectors) or Mantel test (between distance matrices). The PLS-related analysis was performed using the *ropls* package in R (ref. 84) and the Mantel test using the *vegan* package⁷⁵. A list of potential predictors (independent variables, X) for each factor (dependent variable, Y) tested by PLS is included in Supplementary Table 9.

$$R_{PLSj}^2 = R_Y^2 \times \frac{\sum_f (W_{jf}^2 \times SSY_f)}{SSY_{cum}} = \frac{\sum_f (W_{jf}^2 \times SSY_f)}{SSY} \quad (1)$$

where R_{PLSj}^2 is the partial R^2 of variable j based on PLS,
 W_{jf} is the PLS weight of variable j on component f ,
 SSY_f is the sum of squares of Y explained by component f ,
 SSY_{cum} is the cumulative sum of squares of Y explained by all components,
 R_Y^2 is the percentage of Y dispersion (that is, sum of squares) explained by the PLS model and
 SSY is the Y dispersion, that is, sum of squares of Y .

Reporting summary

Further information on research design is available in the Nature Portfolio Reporting Summary linked to this article.

Data availability

The DNA sequences of the archaeal 16S rRNA gene amplicons are available in the National Center for Biotechnology Information (NCBI) Sequence Read Archive under project accession number [PRJNA861672](https://www.ncbi.nlm.nih.gov/submit/PRJNA861672). The DNA sequences of the bacterial 16S rRNA gene amplicons are under the project accession number [PRJNA331185](https://www.ncbi.nlm.nih.gov/submit/PRJNA331185). Raw shotgun metagenomic sequences are deposited in the European Nucleotide Archive

(<http://www.ebi.ac.uk/ena>) under study no. [PRJNA533082](https://www.ncbi.nlm.nih.gov/submit/PRJNA533082). The soil physical and chemical attributes, and plant biomass and richness are downloadable online at <http://www.ou.edu/ieg/publications/datasets>. Silva 132 Ref NR database is available at <https://www.arb-silva.de/documentation/release-132/>. The Greengene reference dataset is available from the QIIME GitHub repository https://github.com/biocore/qiime-default-reference/blob/master/qiime_default_reference/gg_13_8_otus/rep_set/97_otus.fasta.gz. Source data are provided with this paper.

Code availability

R scripts for statistical analyses and source data are available on GitHub at <https://github.com/yazhang2022/OKwarmingSiteArchaea>.

References

- Guo, X. et al. Gene-informed decomposition model predicts lower soil carbon loss due to persistent microbial adaptation to warming. *Nat. Commun.* **11**, 4897 (2020).
- Frank, D. A. & McNaughton, S. J. Aboveground biomass estimation with the canopy intercept method: a plant growth form caveat. *Oikos* **57**, 57–60 (1990).
- Sherry, R. A. et al. Lagged effects of experimental warming and doubled precipitation on annual and seasonal aboveground biomass production in a tallgrass prairie. *Glob. Change Biol.* **14**, 2923–2936 (2008).
- Zhou, J. Z. et al. Microbial mediation of carbon-cycle feedbacks to climate warming. *Nat. Clim. Change* **2**, 106–110 (2012).
- Li, D., Zhou, X., Wu, L., Zhou, J. & Luo, Y. Contrasting responses of heterotrophic and autotrophic respiration to experimental warming in a winter annual-dominated prairie. *Glob. Change Biol.* **19**, 3553–3564 (2013).
- Zhou, J., Bruns, M. A. & Tiedje, J. M. DNA recovery from soils of diverse composition. *Appl. Environ. Microbiol.* **62**, 316–322 (1996).
- Wu, L. et al. Phasing amplicon sequencing on Illumina Miseq for robust environmental microbial community analysis. *BMC Microbiol.* **15**, 125 (2015).
- Caporaso, J. G. et al. Ultra-high-throughput microbial community analysis on the Illumina HiSeq and MiSeq platforms. *ISME J.* **6**, 1621–1624 (2012).
- Suzuki, M. T. & Giovannoni, S. J. Bias caused by template annealing in the amplification of mixtures of 16S rRNA genes by PCR. *Appl. Environ. Microbiol.* **62**, 625–630 (1996).
- Takai, K. & Horikoshi, K. Rapid detection and quantification of members of the archaeal community by quantitative PCR using fluorogenic probes. *Appl. Environ. Microbiol.* **66**, 5066–5072 (2000).
- Porat, I. et al. Characterization of archaeal community in contaminated and uncontaminated surface stream sediments. *Microb. Ecol.* **60**, 784–795 (2010).
- Francis, C. A., Roberts, K. J., Beman, J. M., Santoro, A. E. & Oakley, B. B. Ubiquity and diversity of ammonia-oxidizing archaea in water columns and sediments of the ocean. *Proc. Natl Acad. Sci. USA* **102**, 14683–14688 (2005).
- Peiffer, J. A. et al. Diversity and heritability of the maize rhizosphere microbiome under field conditions. *Proc. Natl Acad. Sci. USA* **110**, 6548–6553 (2013).
- Giardine, B. et al. Galaxy: a platform for interactive large-scale genome analysis. *Genome Res.* **15**, 1451–1455 (2005).
- Kong, Y. Btrim: a fast, lightweight adapter and quality trimming program for next-generation sequencing technologies. *Genomics* **98**, 152–153 (2011).
- Magoc, T. & Salzberg, S. L. FLASH: fast length adjustment of short reads to improve genome assemblies. *Bioinformatics* **27**, 2957–2963 (2011).

64. Edgar, R. C. UPARSE: highly accurate OTU sequences from microbial amplicon reads. *Nat. Methods* **10**, 996–998 (2013).
65. Caporaso, J. G. et al. QIIME allows analysis of high-throughput community sequencing data. *Nat. Methods* **7**, 335–336 (2010).
66. DeSantis, T. Z. et al. Greengenes, a chimera-checked 16S rRNA gene database and workbench compatible with ARB. *Appl. Environ. Microbiol.* **72**, 5069–5072 (2006).
67. Wang, Q., Garrity, G. M., Tiedje, J. M. & Cole, J. R. Naive Bayesian classifier for rapid assignment of rRNA sequences into the new bacterial taxonomy. *Appl. Environ. Microbiol.* **73**, 5261–5267 (2007).
68. Edgar, R. C. UNOISE2: improved error-correction for Illumina 16S and ITS amplicon sequencing. Preprint available at *bioRxiv* <https://doi.org/10.1101/081257> (2016).
69. Callahan, B. J. et al. DADA2: high-resolution sample inference from Illumina amplicon data. *Nat. Methods* **13**, 581–583 (2016).
70. Amir, A. et al. Deblur rapidly resolves single-nucleotide community sequence patterns. *mSystems* **2**, e00191-16 (2017).
71. Kembel, S. W. et al. Picante: R tools for integrating phylogenies and ecology. *Bioinformatics* **26**, 1463–1464 (2010).
72. Sievers, F. et al. Fast, scalable generation of high-quality protein multiple sequence alignments using Clustal Omega. *Mol. Syst. Biol.* **7**, 539 (2011).
73. Price, M. N., Dehal, P. S. & Arkin, A. P. FastTree 2—approximately maximum-likelihood trees for large alignments. *PLoS ONE* **5**, e9490 (2010).
74. Munoz, R. et al. Release LTPs104 of the All-Species Living Tree. *Syst. Appl. Microbiol.* **34**, 169–170 (2011).
75. Oksanen, J. et al. *Package ‘vegan’*. *Community Ecology Package, Version 2.9*, 1–295 (The R Project for Statistical Computing, 2013).
76. Chen, L. X. et al. Comparative metagenomic and metatranscriptomic analyses of microbial communities in acid mine drainage. *ISME J.* **9**, 1579–1592 (2015).
77. Nakagawa, S. & Schielzeth, H. A general and simple method for obtaining R^2 from generalized linear mixed-effects models. *Methods Ecol. Evol.* **4**, 133–142 (2013).
78. Martiny, J. B., Eisen, J. A., Penn, K., Allison, S. D. & Horner-Devine, M. C. Drivers of bacterial beta-diversity depend on spatial scale. *Proc. Natl Acad. Sci. USA* **108**, 7850–7854 (2011).
79. Andrews, S. *FastQC: A Quality Control Tool for High Throughput Sequence Data* (Babraham Bioinformatics, 2010).
80. Li, W. & Godzik, A. Cd-hit: a fast program for clustering and comparing large sets of protein or nucleotide sequences. *Bioinformatics* **22**, 1658–1659 (2006).
81. Patel, R. K. & Jain, M. NGS QC Toolkit: a toolkit for quality control of next generation sequencing data. *PLoS ONE* **7**, e30619 (2012).
82. Zhou, J. Z. & Ning, D. L. Stochastic community assembly: does it matter in microbial ecology? *Microbiol. Mol. Biol. Rev.* **81**, e00002-17 (2017).
83. Jaumot, J., Bedia, C. & Tauler, R. *Data Analysis for Omic Sciences: Methods and Applications* (Elsevier, 2018).
84. Thevenot, E. A., Roux, A., Xu, Y., Ezan, E. & Junot, C. Analysis of the human adult urinary metabolome variations with age, body mass index, and gender by implementing a comprehensive workflow for univariate and OPLS statistical analyses. *J. Proteome Res.* **14**, 3322–3335 (2015).

Acknowledgements

We thank all former and current members of the Institute for Environmental Genomics for their time and energy in maintaining the long-term climate change experiment. This work was supported by the US Department of Energy, Office of Science, Genomic Science Program under Award Number DE-SC0004601 and DE-SC0010715, and the Office of the Vice President for Research at the University of Oklahoma. The data analysis performed by D.N. and N.X. was also partially supported by NSF Grants EF-2025558 and DEB-2129235.

Author contributions

All authors contributed intellectual input and assistance to this study. The original concepts were conceived by Y.Z. and J.Z. Field management was carried out by Y.Z., Linwei Wu, M.M.Y., X.Z., X.G., S.J., Z.Y., S.H., J.F., J.K., C.R.C., C.T.B., Y. Fan, J.P.M., Y.O., Y. Fu, D.N., Z.S., N.X., A.Z. and Liyou Wu. Sample collection, soil chemical and microbial characterization were carried out by Y.H., M.M.Y., Linwei Wu, J.G. and Z.G. Data analyses were done by Y.Z. and D.N. with assistance from Linwei Wu and J.Z. All data analysis and integration were guided by J.Z. The manuscript was prepared by Y.Z., D.N., X.L., Y.Y., J.M.T. and J.Z.

Competing interests

The authors declare no competing interests.

Additional information

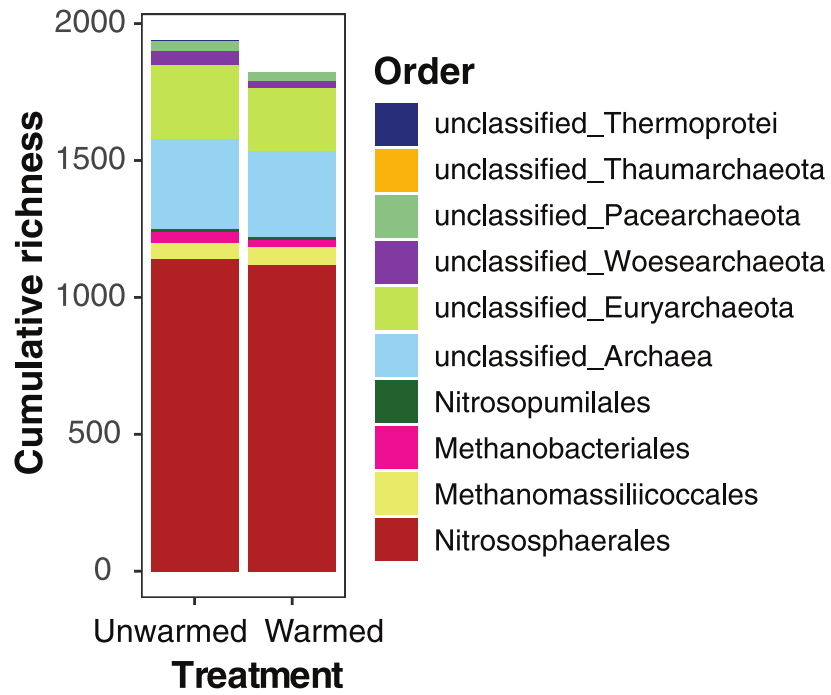
Extended data is available for this paper at <https://doi.org/10.1038/s41558-023-01664-x>.

Supplementary information The online version contains supplementary material available at <https://doi.org/10.1038/s41558-023-01664-x>.

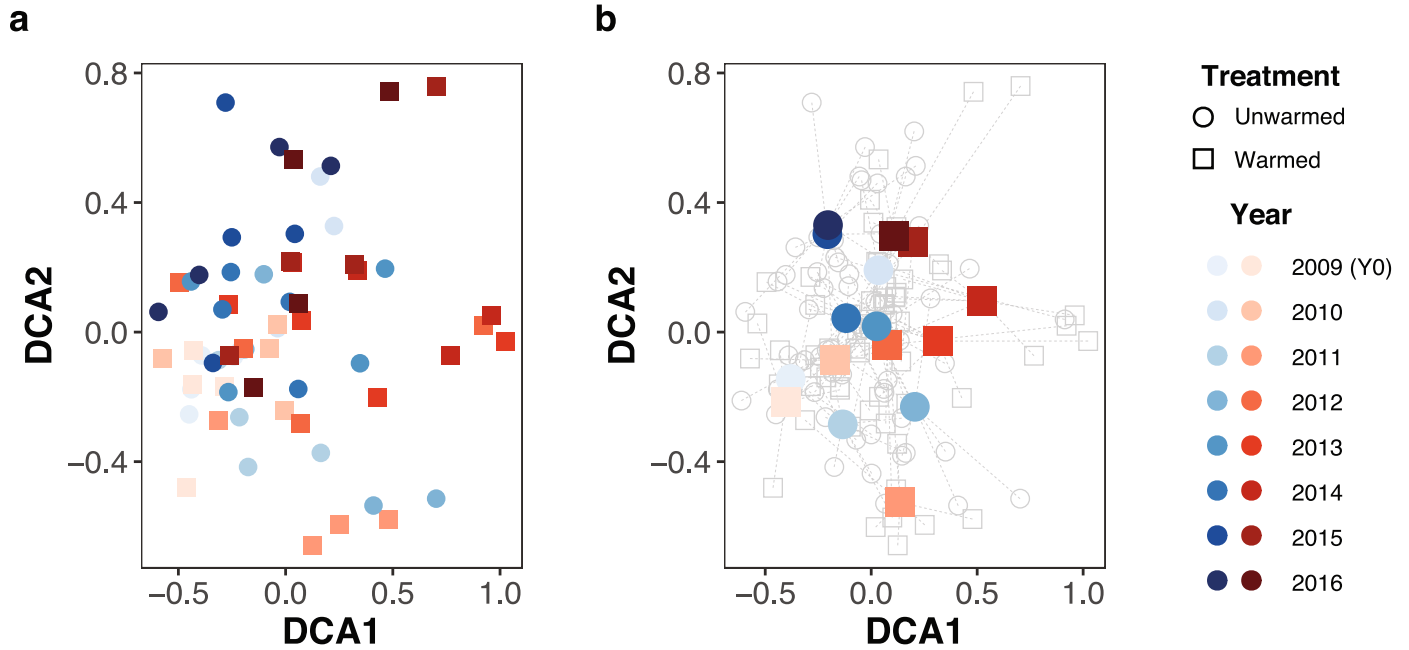
Correspondence and requests for materials should be addressed to Jizhong Zhou.

Peer review information *Nature Climate Change* thanks Federica D’Alò and the other, anonymous, reviewer(s) for their contribution to the peer review of this work.

Reprints and permissions information is available at www.nature.com/reprints.

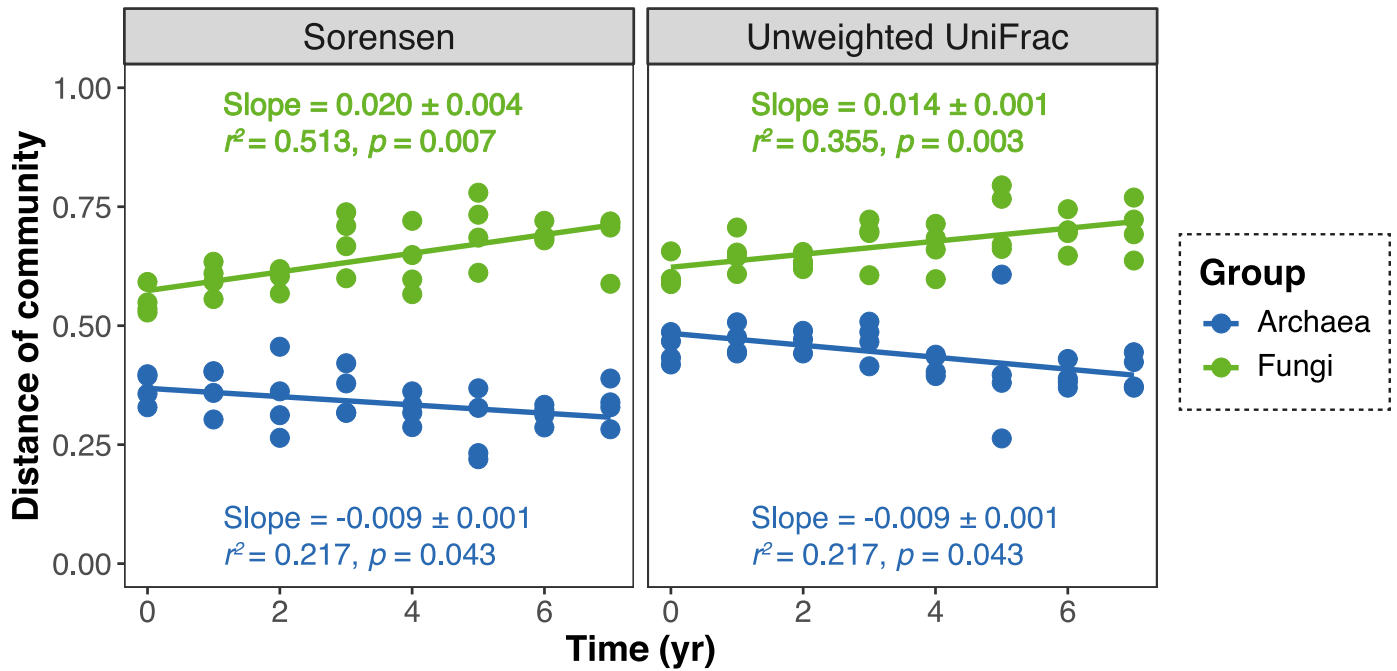


Extended Data Fig. 1 | Effects of experimental warming on archaeal community composition under unwarmed and warmed conditions at the order level. Cumulative richness is expressed as the number of operational taxonomic units (OTUs).



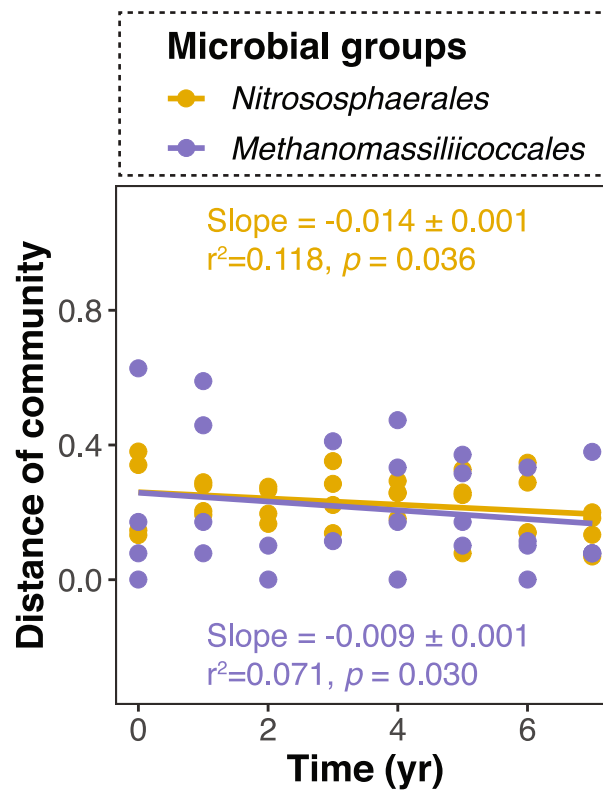
Extended Data Fig. 2 | The succession of soil archaea communities under unwarmed and warmed treatments by detrended correspondence analysis (DCA). Individual samples from warmed and unwarmed plots within each year are shown in (a) and the centroids of four replicates from each treatment within

each year are shown in (b). The analysis was performed based on Sorensen dissimilarity metric. Warmed samples are clustered together with control samples in year 0 (2009) and separated from control samples in the following seven years (2010–2016).



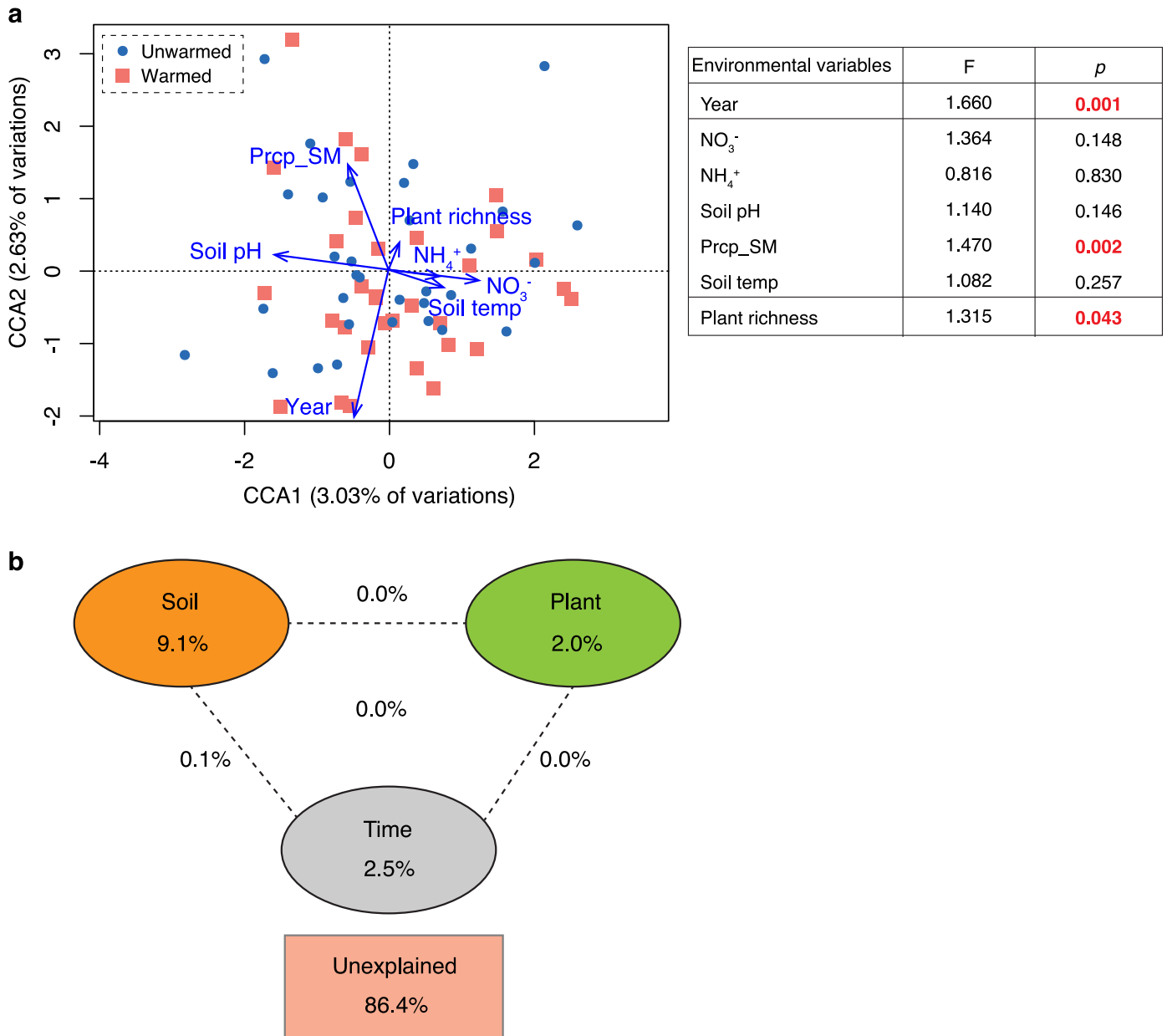
Extended Data Fig. 3 | Temporal changes in community differences between warming and control conditions for archaea and fungi. The first year is 2009 (year 0). Considering the repeated-measures design, the warming-versus-control dissimilarity values at each block were fitted to the linear mixed-effects (LMMs) models with a fixed effect of time and a random intercept and slope effect among

different pairs of plots (blocks). The slopes are presented as a coefficient in fixed effect \pm standard error in random effect. The r^2 values are calculated (details in Methods), reflecting the variance explained by the whole LMM model. p values were based on permutation tests (two-sided). The lines showed the fixed effects of the LMM.



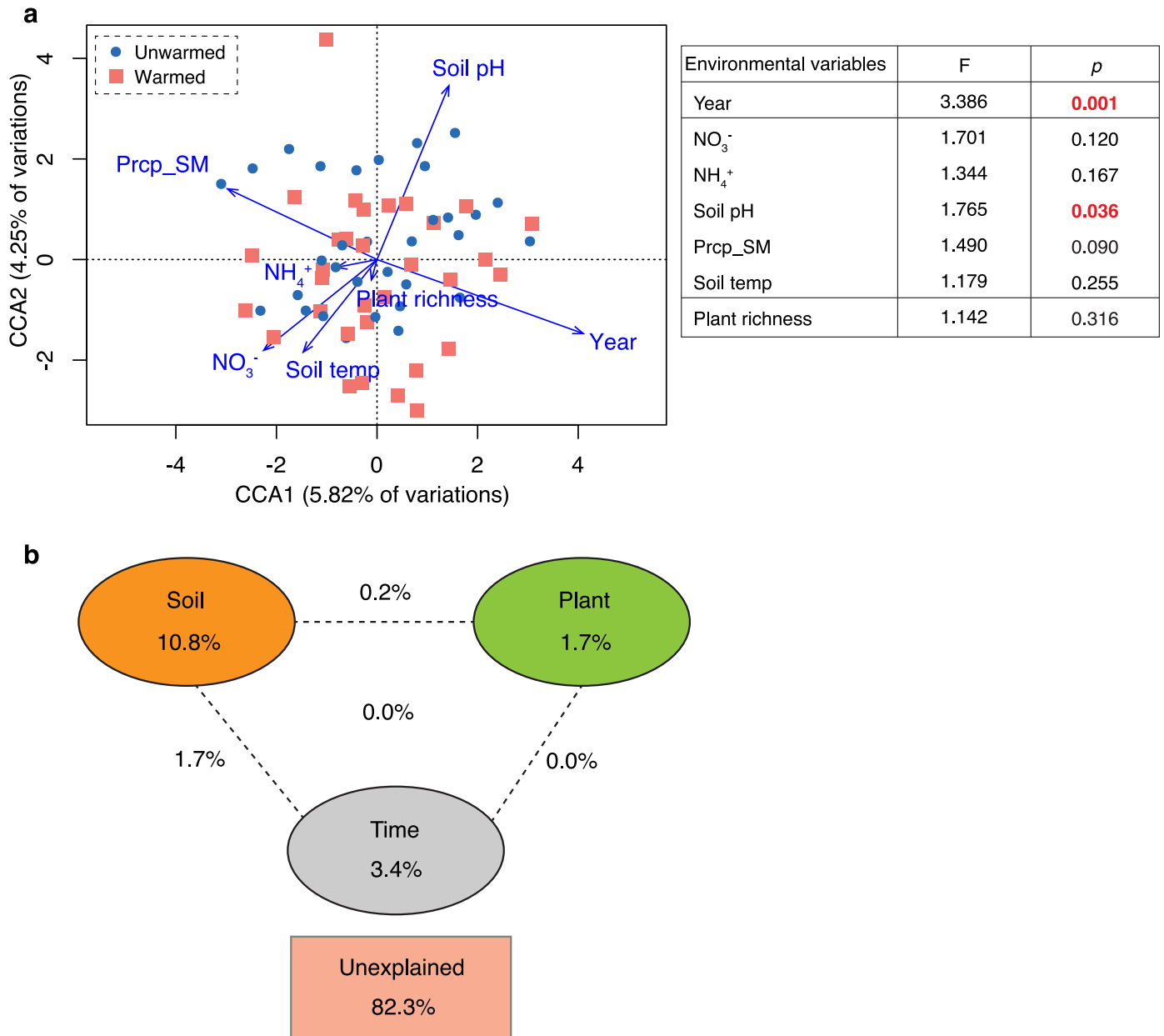
Extended Data Fig. 4 | Temporal changes in community differences between warming and control conditions for orders *Nitrososphaerales* and *Methanomassiliicoccales*. The analysis was performed based on unweighted UniFrac metrics. Considering the repeated-measures design, the warming-versus-control dissimilarity values at each block were fitted to LMMs with a fixed effect of time and a random intercept and slope effect among

different pairs of plots (blocks). The slopes are presented as a coefficient in fixed effect \pm standard error in random effect. The r^2 values are calculated (details in Methods), reflecting the variance explained by the whole LMM model. p values were based on permutation tests (two-sided). The lines showed the fixed effects of the LMM.



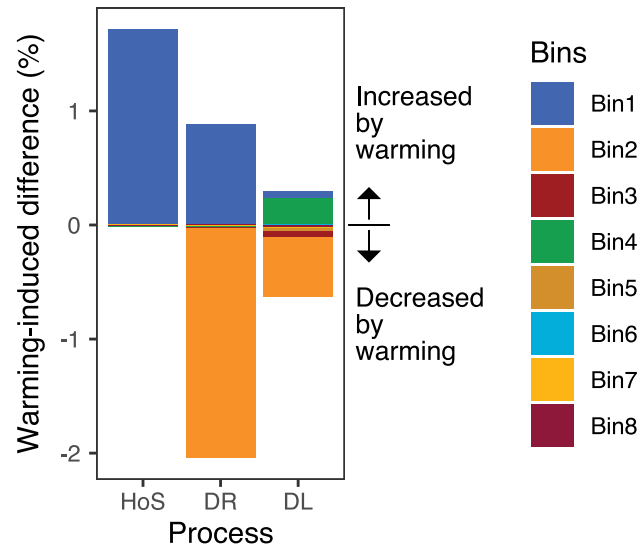
Extended Data Fig. 5 | Constrained ordination analysis of archaeal communities. (a) Canonical correspondence analyses (CCA) of soil archaea community and environmental attributes. Tested environmental attributes include soil nitrate (NO₃⁻), ammonium (NH₄⁺), total nitrogen (TN), total organic C (TOC), pH, Precipitation of sampling month (Prcp_SM), temperature, moisture drought index, C₃ and C₄ aboveground biomass, plant richness, and total biomass. The insert table shows the significance of each environmental variable

in explaining the variations of archaeal community (one-way ANOVA test). (b) CCA-based variation partitioning analysis (VPA) showed the relative proportions of archaeal community variations that can be explained by different types of environmental factors. The numbers within the circles showed the variation explained by each group of environmental factors alone. The numbers between the circles showed the interactions of the two factors on either side and number in the center of the interactions of all three factors.

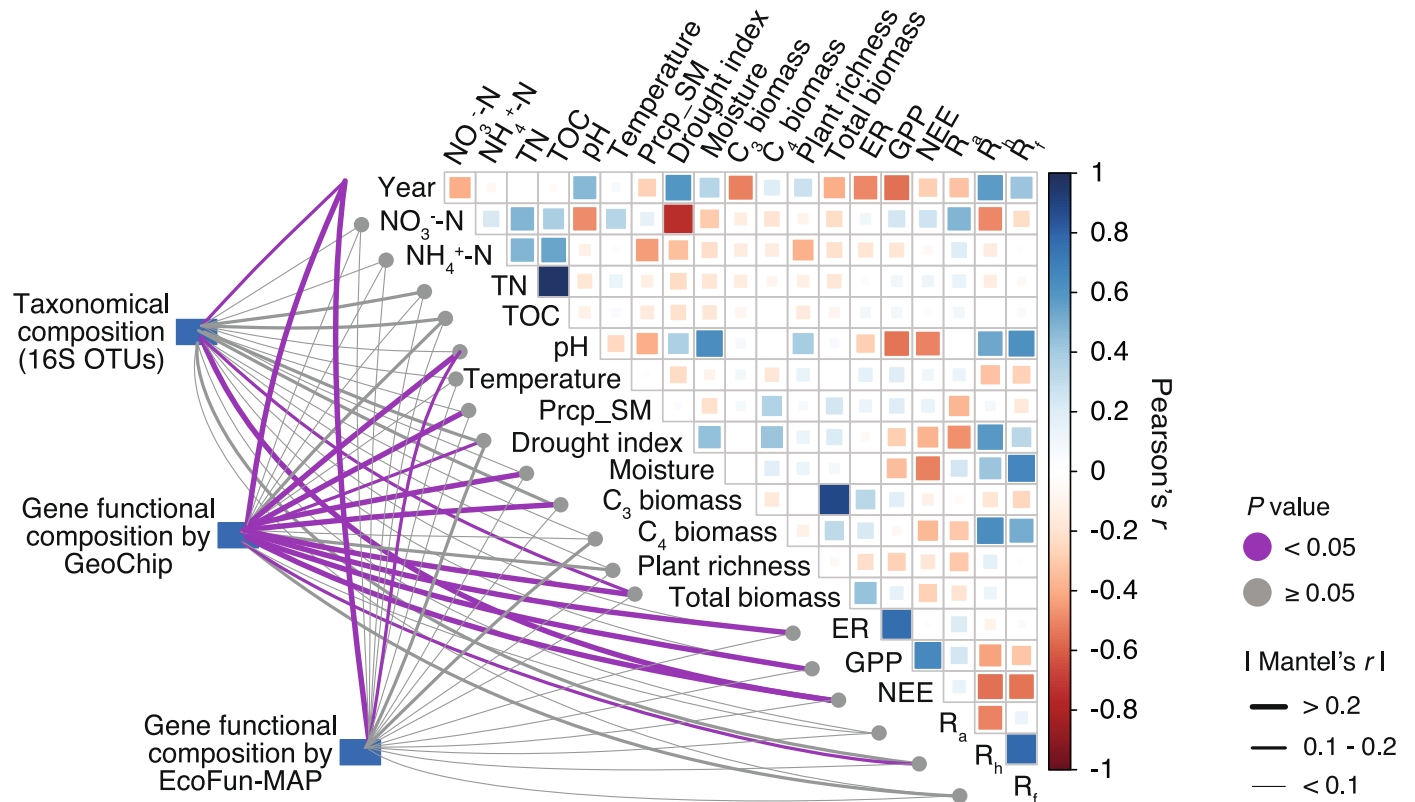


Extended Data Fig. 6 | Constrained ordination analysis of the order *Nitrososphaerales*. (a) CCA of the *Nitrososphaerales* group and environmental attributes. The tested environmental attributes and other properties are the same as in Extended Data Fig. 5 (one-way ANOVA test). Significant tests ($P < 0.05$) are shown in bold red. (b) CCA-based VPA showed the relative proportions of

variations in the *Nitrososphaerales* group that can be explained by different types of environmental factors. The numbers within the circles showed the variation explained by each group of environmental factors alone. The numbers between the circles showed the interactions of the two factors on either side and number in the center of the interactions of all three factors.



Extended Data Fig. 7 | Warming-induced changes of different bins. Warming-induced difference between warming and control is expressed in percentages for the three dominating ecological processes—homogeneous selection (HoS), dispersal limitation (DL), and drift and others (DR).



Extended Data Fig. 8 | Relationships between archaeal community structure and environmental variables and ecosystem processes under control. Archaeal community structures, which include taxonomical composition by

16 S rRNA genes and functional gene composition by GeoChip and EcoFUN-MAP, were tested against time, soil and plant variables and ecosystem C fluxes. All the other properties are the same as Fig. 4a.

Reporting Summary

Nature Portfolio wishes to improve the reproducibility of the work that we publish. This form provides structure for consistency and transparency in reporting. For further information on Nature Portfolio policies, see our [Editorial Policies](#) and the [Editorial Policy Checklist](#).

Statistics

For all statistical analyses, confirm that the following items are present in the figure legend, table legend, main text, or Methods section.

- | n/a | Confirmed |
|-------------------------------------|--|
| <input type="checkbox"/> | <input checked="" type="checkbox"/> The exact sample size (n) for each experimental group/condition, given as a discrete number and unit of measurement |
| <input type="checkbox"/> | <input checked="" type="checkbox"/> A statement on whether measurements were taken from distinct samples or whether the same sample was measured repeatedly |
| <input type="checkbox"/> | <input checked="" type="checkbox"/> The statistical test(s) used AND whether they are one- or two-sided
<i>Only common tests should be described solely by name; describe more complex techniques in the Methods section.</i> |
| <input type="checkbox"/> | <input checked="" type="checkbox"/> A description of all covariates tested |
| <input type="checkbox"/> | <input checked="" type="checkbox"/> A description of any assumptions or corrections, such as tests of normality and adjustment for multiple comparisons |
| <input type="checkbox"/> | <input checked="" type="checkbox"/> A full description of the statistical parameters including central tendency (e.g. means) or other basic estimates (e.g. regression coefficient) AND variation (e.g. standard deviation) or associated estimates of uncertainty (e.g. confidence intervals) |
| <input type="checkbox"/> | <input checked="" type="checkbox"/> For null hypothesis testing, the test statistic (e.g. F , t , r) with confidence intervals, effect sizes, degrees of freedom and P value noted
<i>Give P values as exact values whenever suitable.</i> |
| <input checked="" type="checkbox"/> | <input type="checkbox"/> For Bayesian analysis, information on the choice of priors and Markov chain Monte Carlo settings |
| <input checked="" type="checkbox"/> | <input type="checkbox"/> For hierarchical and complex designs, identification of the appropriate level for tests and full reporting of outcomes |
| <input type="checkbox"/> | <input checked="" type="checkbox"/> Estimates of effect sizes (e.g. Cohen's d , Pearson's r), indicating how they were calculated |

Our web collection on [statistics for biologists](#) contains articles on many of the points above.

Software and code

Policy information about [availability of computer code](#)

Data collection

Data analysis

For manuscripts utilizing custom algorithms or software that are central to the research but not yet described in published literature, software must be made available to editors and reviewers. We strongly encourage code deposition in a community repository (e.g. GitHub). See the Nature Portfolio [guidelines for submitting code & software](#) for further information.

Data

Policy information about [availability of data](#)

All manuscripts must include a [data availability statement](#). This statement should provide the following information, where applicable:

- Accession codes, unique identifiers, or web links for publicly available datasets
- A description of any restrictions on data availability
- For clinical datasets or third party data, please ensure that the statement adheres to our [policy](#)

The DNA sequences of the archaeal 16S rRNA gene amplicons are available in the National Center for Biotechnology Information (NCBI) Sequence Read Archive under project accession number PRJNA861672. The DNA sequences of the bacterial 16S rRNA gene amplicons were under the project accession number PRJNA331185. Raw shotgun metagenomic sequences are deposited in the European Nucleotide Archive (<http://www.ebi.ac.uk/ena>) under study no. PRJNA533082. The soil physical and chemical attributes, and plant biomass and richness are downloadable online at <http://www.ou.edu/ieg/publications/datasets>. Silva 132 Ref NR database is available at <https://www.arb-silva.de/documentation/release-132/>. Greengene reference data set is available from the QIIME github repository https://github.com/biocore/qiime-default-reference/blob/master/qiime_default_reference/gg_13_8_otus/rep_set/97_otus.fasta.gz. Source data are provided with this paper.

Human research participants

Policy information about [studies involving human research participants and Sex and Gender in Research](#).

Reporting on sex and gender	<input type="text" value="Not applicable"/>
Population characteristics	<input type="text" value="Not applicable"/>
Recruitment	<input type="text" value="Not applicable"/>
Ethics oversight	<input type="text" value="Not applicable"/>

Note that full information on the approval of the study protocol must also be provided in the manuscript.

Field-specific reporting

Please select the one below that is the best fit for your research. If you are not sure, read the appropriate sections before making your selection.

- Life sciences Behavioural & social sciences Ecological, evolutionary & environmental sciences

For a reference copy of the document with all sections, see [nature.com/documents/nr-reporting-summary-flat.pdf](https://www.nature.com/documents/nr-reporting-summary-flat.pdf)

Ecological, evolutionary & environmental sciences study design

All studies must disclose on these points even when the disclosure is negative.

Study description	The field experiment was conducted at the Kessler Atmospheric and Ecological Field Station (KAEFS) of the US Great Plain in McClain County, Oklahoma, USA (34 59' N, 97 31'W). This experiment used a blocked split-plot design, in which warming (continuous heating at a target of +3 °C above ambient) was the primary factor. Thus, this experiment has two different treatment groups (warming versus control). Each of these treatments has 4 replicates in different four blocks, that is, a total of eight plots.
Research sample	Before the experiment started (i.e., year 2009), eight pre-warmed surface (0 - 15 cm) soil samples were collected using a soil core as the background of comparison. For the following years (i.e., from year 2010 to 2016), a total of 56 samples were collected during the experiment, one sample per plot per year. With the blocked split-plot design of the experimental site, annual soil samples were taken in peak growth season from warming (continuous heating at a target of +3 °C above ambient) and control plots. Soil microbial DNA was extracted from 1.5 g of well-mixed soil for each sample in order to investigate the richness and abundance distribution of microbial (e.g., archaeal and bacterial) communities over the years.
Sampling strategy	Sampling strategy was determined together with the site design. With the two treatment groups of the study site (see details in Study description), 4 biological replicates located in each of the 4 blocks for each treatment were sampled annually (from 2010 to 2016). These 64 samples from the two treatment groups would be sufficient for measuring variation and evaluating differences in and between treatments using statistical tests, such as linear mixed-effects models. The surface (0 - 15cm) soil samples were taken using a standard soil corer (2.5 cm in diameter). About 50 g of soil sampled were mixed well before 1.5 g of soil was weighed for DNA extraction from each plot/timepoint.
Data collection	Soil temperature was measured every 15 min at depth of 7.5, 20, 45 and 75 cm in the center of each plot using constantan-copper thermocouples wired to a Campbell Scientific CR10x data logger (Campbell Scientific). The data were recorded and backed up by Daliang Ning in computers periodically. Soil chemical properties, including total carbon (C), total nitrogen (N), nitrate (NO ₃ ⁻) and ammonia (NH ₄ ⁺), were analyzed in the Soil, Water, and Forage Analytical Laboratory at Oklahoma State University (Stillwater, OK,

USA). The results were sent to Linwei Wu through emails and stored in computers. Volumetric soil water content (%V) was measured using a portable time domain reflectometer (Soil Moisture Equipment Corp.) once or twice a month, and recorded by pen and paper. Ecosystem carbon (C) fluxes were measured once or twice a month between 10:00 and 15:00 (local time). Net ecosystem exchange and ecosystem respiration were measured using an LI-6400 portable photosynthesis system (LI-COR) attached to a transparent chamber (0.5m×0.5m×0.7m), which covered all of the vegetation within the aluminium frames. The LI-6400 system had storage to record the data. Soil total respiration and heterotrophic respiration were measured using a LI-8100A soil flux system attached to a soil CO₂ flux chamber (LI-COR). The LI-8100A system had storage to record the data. Meanwhile, a manual record (by pen and paper) was also kept. Soil water content and ecosystem carbon fluxes were measured monthly or biweekly by the field team, including Ya Zhang, Linwei Wu, Mengting Maggie Yuan, Xishu Zhou, Xue Guo, Siyang Jian, Zhifeng Yang, Shun Han, Jiajie Feng, Jialiang Kuang, Carolyn R. Cornell, Colin T. Bates, Yupeng Fan, Jonathan P. Michael, Yang Ouyang, Ying Fu, Daliang Ning, Zheng Shi, Naijia Xiao, Aifen Zhou, and Liyou Wu. Amplicon sequencing was performed following a published protocol (Wu 2015) on Illumina MiSeq platform.

Timing and spatial scale	The experimental site was initiated in July of 2009. Data and samples for this study were collected since then to 2016 (ending date: Dec 22, 2016). The samples/data collected in 2009 were used the background of comparison (before the experiment started) and the samples/data collected in the following years 2010-2016 were during the warming experiments. This study was to investigate the richness and abundance distribution of microbial (e.g., archaeal and bacterial) communities over the years. Therefore, one soil sample were collected in each plot once every year. Soil temperature was measured every 15min at depth 7.5 cm and annual average values of temperature were used to represent soil temperature across experimental years. Volumetric soil water content (% V) was measured once or twice a month, and annual average values were used to represent soil moisture. Ecosystem carbon (C) fluxes were measured once or twice a month between 10:00 and 15:00 (local time) and annual average values were used in analyses. There were no gaps between collection periods. The site has four experimental blocks, each including six plots. Each plot has the size of 2.5×3.5m ² .
Data exclusions	No data were excluded.
Reproducibility	Our data were from 4 biological replicates located in each of the 4 blocks for the warming treatment (spatially). They were time series data collected annually from 2009-2016 (temporally). There were no temporal replications. All the attempts at replicates were successful.
Randomization	The plots within each block were assigned to different treatments randomly.
Blinding	All the soil sample processing and field measurements were done following the same way, and without signs/labels noting the relevant treatment.
Did the study involve field work?	<input checked="" type="checkbox"/> Yes <input type="checkbox"/> No

Field work, collection and transport

Field conditions	The field experiment was conducted at the Kessler Atmospheric and Ecological Field Station (KAEFS) of the US Great Plain in McClain County, Oklahoma, USA (34 59' N, 97 31'W). The average air temperature was 16.3 °C and the average annual precipitation was 914 mm, based on Oklahoma Climatological Survey from 1948 to 1999. The experimental site was dominated by C3 forbs (Solanum carolinense, Ambrosia trifida and Euphorbia dentate), C3 grasses (Bromus sps) and C4 grasses (Tridens flavus and Sorghum halapense). The soil type was Port-Pulaski-Keokuk complex, with a neutral pH, a high available water holding capacity (37%) and a deep (ca. 70 cm), moderately penetrable root zone.
Location	The field experiment was conducted at the Kessler Atmospheric and Ecological Field Station (KAEFS) of the US Great Plain in McClain County, Oklahoma, USA (34 59' N, 97 31'W). See KAEFS website for more details (https://www.ou.edu/kaefs).
Access & import/export	The property on which the field experiment was built belongs to the University of Oklahoma. The acting director of the site is Meghan Bomgraars (mbomgraars@ou.edu, 405-325-5202). The authors have full access to the field site to conduct research. All the research activities conducted on site complies to national and local laws and regulations, and rules imposed by the University of Oklahoma in terms of ecological conservation and work safety.
Disturbance	The field experimental site was fenced with a buffer area without significant disturbance to the tall grass prairie around.

Reporting for specific materials, systems and methods

We require information from authors about some types of materials, experimental systems and methods used in many studies. Here, indicate whether each material, system or method listed is relevant to your study. If you are not sure if a list item applies to your research, read the appropriate section before selecting a response.

Materials & experimental systems

- | n/a | Included in the study |
|-------------------------------------|--|
| <input checked="" type="checkbox"/> | <input type="checkbox"/> Antibodies |
| <input checked="" type="checkbox"/> | <input type="checkbox"/> Eukaryotic cell lines |
| <input checked="" type="checkbox"/> | <input type="checkbox"/> Palaeontology and archaeology |
| <input checked="" type="checkbox"/> | <input type="checkbox"/> Animals and other organisms |
| <input checked="" type="checkbox"/> | <input type="checkbox"/> Clinical data |
| <input checked="" type="checkbox"/> | <input type="checkbox"/> Dual use research of concern |

Methods

- | n/a | Included in the study |
|-------------------------------------|---|
| <input checked="" type="checkbox"/> | <input type="checkbox"/> ChIP-seq |
| <input checked="" type="checkbox"/> | <input type="checkbox"/> Flow cytometry |
| <input checked="" type="checkbox"/> | <input type="checkbox"/> MRI-based neuroimaging |